Republic of Iraq
Ministry of Higher Education
and Scientific Research
University of Baghdad
College of Pharmacy

Formulation and *In-vitro* Characterization of Nefopam Hydrochloride as In-situ nasal gel

A Thesis

Submitted to the Department of Pharmaceutics and the Committee of Post Graduate Studies of the College of Pharmacy/University of Baghdad in Partial Fulfillment of the Requirements for the Degree of Master in Science of Pharmacy "Pharmaceutics"

By

Ammar Abdulmajeed Ahmed Alabdly

B.Sc. Pharmacy

(2016)

Supervised by

Assist Prof. Dr. Hanan Jalal Kassab

2022 A.D **1444 A.H**

بسم الله الرحمن الرحيم

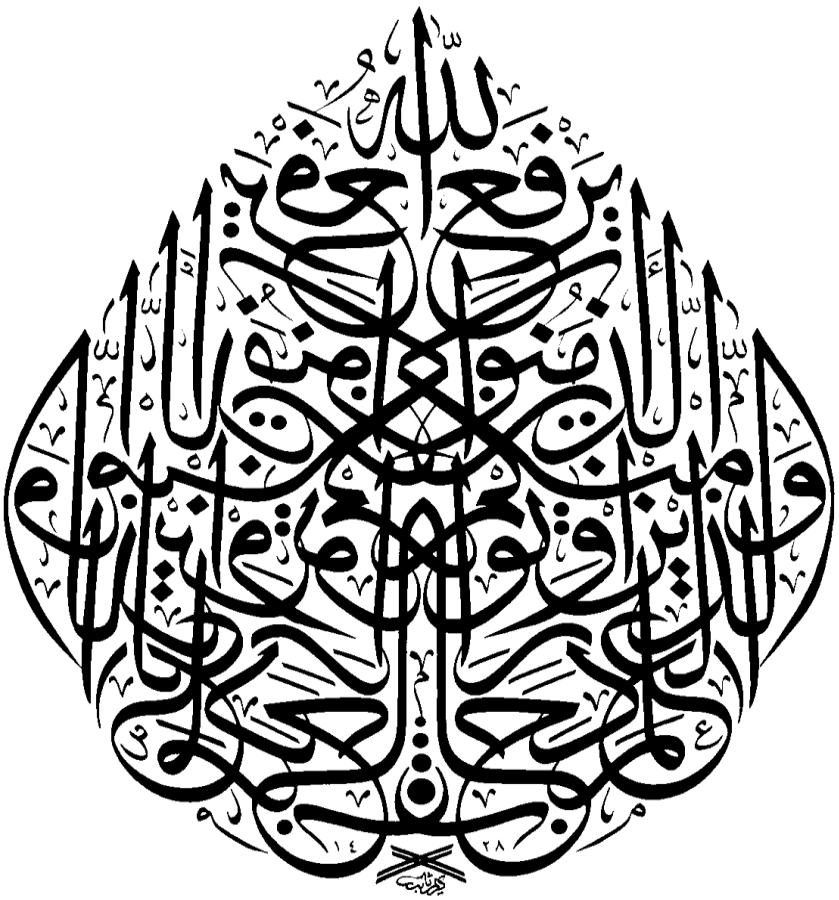

سورة المجادلة – آية ١١

Supervisor Certificate

I certify that this thesis titled**, "Formulation and *In-vitro* Characterization of Nefopam Hydrochloride as In-situ nasal gel"** was prepared under my supervision at the University of Baghdad, College of Pharmacy as a partial fulfillment of the requirements for the degree of Master in Science of Pharmacy (Pharmaceutics).

Signature:
Advisor: ***Assist Prof. Dr. Hanan Jalal Kassab***
Department: Pharmaceutics
College of Pharmacy/University of Baghdad
Date: / / 2022

In view of the available recommendation, I forward this thesis for the debate by the examining committee

Signature:
Name: ***Assist. Prof. Dr. Munaf H. Zalzala***
Assistant Dean for Scientific and Students Affairs in the College of Pharmacy/University of Baghdad
Date: / /2022

Certificate of Examination Committee

We, the examining committee after reading this thesis titled, **"Formulation and *In-vitro* Characterization of Nefopam Hydrochloride as In-situ nasal gel"**, and examining the student ***Ammar Abdulmajeed Ahmed Alabdly*** in its contents, found it adequate as a thesis for fulfillment of the requirements for the degree of Master in Science of Pharmacy (Pharmaceutics).

Signature:
Name: ***Assist. Prof. Dr. Entidhar Jassim Mohammed***
(Chairman)
Date: / /2022

Signature:
Name: ***Assist. Prof. Dr. Israa Ghazi Jabbar***
(Member)
Date: / /2022

Signature:
Name: ***Assist. Prof. Eman Beker Hazim***
(Member)
Date: / /2022

Approved by the College of Pharmacy committee for the post graduate studies.

Signature
Name: ***Assist. Prof. Dr. Sarmed H. Kathem***
Dean of the College of Pharmacy / University of Baghdad
Date: / /2022

Dedication

To my mother & father ……

To my lovely wife Enas Alani & my little angel Ruya …….

To my brothers & sister ……

I dedicate this thesis

With love

Ammar

Acknowledgment

Praise is to our almighty gracious Allah for enabling me to finish and present this work.

I would like to express my heartfelt gratitude and appreciation to my supervisor ***Assist Prof. Dr. Hanan Kassab*** without her meticulous supervision and continuous support, this work could never be accomplished.

I wish to express my thanks to ***Assist. Prof. Dr. Sarmed H. Kathem***, the Dean of College of Pharmacy, University of Baghdad, for his generous support.

I would like to express my deepest thanks to ***Assist. Prof. Dr. Munaf H. Zalzala***, the chairman of the committee of graduate studies in the College of Pharmacy, ***Assist. Prof. Dr. Khalid K. Alkinani***, the chairman of the Pharmaceutics Department, for their help and support.

I am so thankful to ***Prof. Dr. Mowafaq M.Ghareeb , Prof. Dr. Nawal Ayash, Prof. Dr. Shaimaa N. Abdulhameed, Assist. Prof. Dr.Fatimaa J. Jawad , and Assist. Prof. Dr.Entidhar J. Mohammed , Assist. Prof. Eman Beker Hazim,*** the members of pharmaceutical department for their valuable help and support during the study.

I would like to thank ***College of Pharmacy, University of Baghdad*** for offering the opportunity to continue my graduate study.

I would like to express my sincere thanks and sincere gratitude to ***All my classmates' friends***, especially to close friends ***Ahmed A. Essa, Othman F. Baker*** for sharing the path and the lab.

I would like also to express my grateful thanks and love to my family and friends and to all others who helped me to finish this work.

Ammar Abdulmajeed Ahmed Alabdly

List of Contents

List of Tables

List of Figures

List of Abbreviations

Abbreviation	Meaning
AIC	Lower Akaike information criterion
API	Active pharmaceutical ingredient
BCS	Biopharmaceutical Classification System
BDDSC	Biopharmaceutical Drug Disposition Classification System
BNZ	Benzalkonium chloride
Car934	Carbopol 934
cgc	Critical gel concentration
cP	Centi poise
Da	Dalton
DSC	Differential Scanning Calorimetry
ECHA	European Chemicals Agency
EMA	European Medicines Agency
FDA	U.S. Food and Drug Administration
FTIR	Fourier Transform Infrared Spectroscopy
GIT	Gastro Intestinal Tract
HA	Hyaluronic acid
HPMC	Hydroxypropyl methylcellulose
I.V	Intravenous
kDa	Killo dalton
LCST	Lower critical solution temperature
MC	Methylcelloluse
NF	Nefopam hydrochloride
OMEs	Odorant-metabolizing enzymes
PAA	Poly(acrylic acid)
PAAm	Poly(acrylamide)
PBS	Phosphate buffer saline
PEO	Poly(ethylene oxide)
PNIPAAm	Poly(N-isopropylacrylamide)
POE	Poly(oxyethylene)
PoloX 188	Poloxamer 188
PoloX 407	Poloxamer 407
POP	Poly(oxypropylene)
PPO	Polo(propylene oxide)
ppt	Precipitate
SD	Standard deviation
SNF	Simulated nasal fluid
Tsol-gel	Gelation temperature
UCST	Upper critical solution temperature
XMEs	Xenobiotic-metabolizing enzymes

Abstract

Nefopam HCl (NF) is a non-narcotic, non-opioid, centrally acting analgesic. It has a limited bioavailability (approximately 36%) as a result of liver first-pass hepatic metabolism.

This study aims to develop and improve mucoadhesive nasal thermosensitive in-situ gel of nefopam hydrochloride to prolong nasal residence time for pain management.

In situ gel of NF formulas (No. 1-48, 20 mg/ml NF) were formulated by the cold approach using different concentrations of thermosensitive Poloxamer 407 alone or with a combination of Poloxamer 188 with a mucoadhesive polymer(s); Hydroxypropyl methylcellulose K4M, Carbopol® 934, Methylcellulose and Hyaluronic acid polymers.

The prepared formulas were subjected to gelation temperature and time, clarity and appearance, and these were the criteria for the initial selection of formulas. The pH, gel strength, drug content, gel spreadability, osmolarity, mucoadhesive force determination, viscosity, and *in-vitro* drug release of formulations was performed, the most suitable formulas were subjected to permeation study, Fourier transform infrared (FTIR) compatibility studies, and stability study.

The results showed that formulas No. (F 13,16,17,20,21,24,41,44,45) passed the initial gelation temperature and gelling capacity and appearance criteria as well as other characterization tests, but only they differentiate in drug release in comparison with a NF aqueous solution as a control.

The formulas No. F21 and 45 (Poloxamer 407 17% and Hyaluronic acid 0.25%, Poloxamer 407 17% and Methylcellulose 0.1%, respectively) show similarity in release pattern in comparison with control.

The formula No. F21 show enhanced *ex-vivo* permeation through sheep nasal mucosa in comparing with control, that attributed to the permeation enhancing effects as well as due to increasing residence time of mucoadhesive polymers.

No interaction between NF and other additives in both formulas, according to FTIR studies.

In conclusion, a promising non-invasive thermosensitive nasal mucoadhesive in situ gel of nefopam hydrochloride can be prepared successfully by using poloxamer 407 based in situ gel together with mucoadhesive polymers.

Chapter One

Introduction

1. Introduction

1.1. Nose-to-brain drug delivery

The brain remains to be one of the most vital, delicate, and intricate organs of the human body, which remains isolated from the regular blood circulation through various protective layers. It is the command center of the body, which regulates almost all the body functions, including involuntary and voluntary functions. It also stores information and sends messages to different body parts. The protective layers, including the skull, and meninges, along with the CSF, Blood-Brain barrier, and blood-CSF barrier, act as a shield for the human brain. These barriers, therefore, preserve the integrity and maintain the homeostasis of the brain and keep it safe from external injuries, shock, trauma, infections, and any other harmful stimuli [(1)].

Several approaches were tried to improve the access of drugs to the brain, including invasive techniques like intracerebroventricular injections, cerebral implants., etc. These showed varying degrees of enhancement in brain availability of drugs but are associated with several limitations and risks [(2)].

William H. Frey II, 1989 discovered the first concept of the intranasal route for the delivery of therapeutically active compounds directly into the CNS. Since then, a remarkable study has been done on the nose-to-brain drug delivery system. Initially, the investigation focused on the nasal delivery of insulin to the brain for the treatment of Alzheimer's disease. Shortly, it was noticed that along with insulin, various other proteins and peptides remain available for efficient delivery to the brain via the nasal route [(3)].

The nose-to-brain pathway is a critical and noninvasive technique for delivering drugs to the brain. The nasal cavity and central nervous system have a well-established nasal anatomical link, implying the development of nasal formulations for brain-targeted [(4)].

Numerous studies have demonstrated kinetic evidence for nose-to-brain targeting by administering intranasally tagged tracers such as albumin and insulin [5].

1.2. Possible mechanisms of nasal to brain drug transportation

Anatomically, the nasal cavity or nose's interior is where breathed air enters the body, forming the first group of respiratory system structures. Two cavities make up the nasal cavity structure, and a mucosal layer completely covers each cavity. The nasal cavity is further split into three main sections: the nasal vestibule, which is the dilated aperture of the nose; the respiratory portion, which refers to the channel for air travel; the olfactory section, which contains the olfactory receptors [6]. The smell of an odorant is perceived by means of these olfactory receptors. The nasal mucosa on the olfactory area does not have small cilia like other parts of the nasal mucosa; instead, it has olfactory neural cells. The olfactory neuroepithelium is structurally distinct as the sole area of the CNS that interacts with the outside world and is capable of regeneration. Therefore, the administration of medications that target the CNS at this olfactory location is suitable. Also, the trigeminal and maxillary nerves innervate the nasal mucosa [7].

Even though the brain's intranasal absorption mechanisms are not fully understood, one method involves the drug being absorbed and transported by a neuronal pathway, like the trigeminal or olfactory nerves, while the other involves lymphatic, vascular, or CSF pathways. One or a combination of mechanisms may be involved in the transportation of drugs from the nasal cavity to the brain [8]. The common feature between these distinct pathways is that they all presuppose the nasal delivery of medications and the partial avoidance of elimination due to enzymatic degradation or the physical clearance mechanisms[9]. However, they differ entirely regarding the drug absorption site and the amount of time required for absorption to occur. The

physicochemical properties of the drug (or the formulation) dominate certain pathways over others [10].

1.2.1. Neuronal pathways

The olfactory and trigeminal pathways are included neuronal pathways; the olfactory pathway consists of the olfactory epithelium, olfactory tract, anterior olfactory nucleus, piriform cortex, amygdala, and hypothalamus. It has been suggested that drugs can reach the CNS via extracellular or intracellular transport along olfactory nerves and that this pathway can be the major route for brain delivery of drugs following nasal administration [9]. Figure 1 shows the mechanism of the olfactory nose-to-brain drug delivery.

The delivered drug needs to cross the olfactory epithelium to be absorbed by olfactory neurons [11]. This absorption is controlled by three mechanisms; passive diffusion, paracellular transport, or endocytosis by neuronal cells. Lipophilic drugs are mostly transported via passive diffusion, whereas paracellular movement is responsible for the transportation of hydrophilic drugs. The lipophilicity and the molecular weight of a drug molecule significantly affect these mechanisms [12].

The trigeminal nerve regulates sensory information from the nasal cavity, oral cavity, and cornea. It innervates the nasal olfactory epithelium at one end, whereas the other end reaches the brain by two different sites; near the pons and cerebrum of the brain, as well as to the frontal brain and olfactory bulb to a lesser extent [5]. Researches showed evidence of delivery of insulin-like-growth factor-I to the CNS via nasal administration through the olfactory and trigeminal pathways [13].

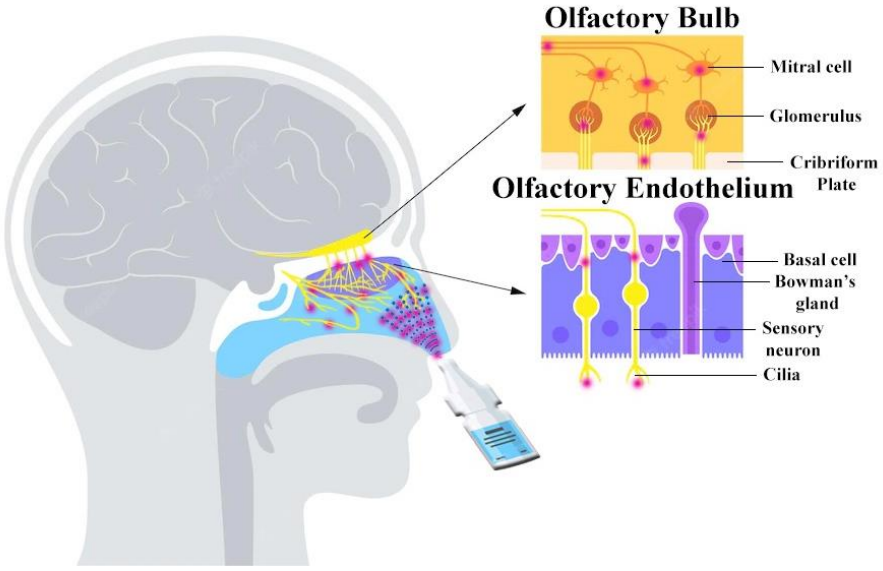

Figure 0. Olfactory route for nose to brain drug administration [9].

1.2.2. Systemic pathways

In addition to direct pathways, the drug can enter the brain indirectly via blood vasculature and/or lymphatic system. The nasal mucosa is highly vascularized, and the blood vessels (lined with continuous and fenestrated endothelium) allow the passage of drugs (in free or may be, even in particle-encapsulated form, following nasal drug administration in nano drug delivery systems). A drug that has become absorbed into the systemic circulation has to cross the BBB in order to reach the CNS. Therefore, the efficiency of this indirect pathway of drug delivery to the brain following nasal administration can differ in the individual patients or depending on the applied disease model [9]. The nasal lymphatic system is connected to the cerebrospinal fluid (CSF) via olfactory nerves [14].

These pathways can probably transport drugs delivered into the nasal cavity to the CSF and perivascular part to distribute to the other part of the brain. Several significant factors and physicochemical characteristics have an impact on the nasal transport and dispersion of drugs: (1) the drug's physiochemical characteristics, such as its molecular weight, particle size, lipophilic-hydrophilic balance, and enzyme degradability; (2) Nasal effect,

including membrane nature, environment, nasal clearance, and (3) Delivery effect, including formulation, drugs distribution and deposition, and viscosity of the formulation [12,15,16].

1.3. Advantages and disadvantages of nasal drug delivery

1.3.1. Advantages of nasal-to-brain drug delivery

The nose-to-brain drug delivery shows several advantages in comparing with the oral and intravenous routes of administration, these advantages including [17–19]:

1- Non-invasive and painless
2- Easiness of application
3- Rapid onset of activity
4- Improve bioavailability by passing hepatic degradation effect, harsh environment of GIT, BBB, plasma protein binding, and reduce the volume of distribution
5- Large surface area for absorption, the volume and the surface area of the nasal cavity are 15-20 ml and 150-200 cm^2, respectively
6- Reduce systemic side effects
7- Nasal administration is advantageous for the management of certain emergency scenarios, such as acute seizure episodes or opioid overdose, because it does not require skilled specialists or a hospital setting
8- Enhance patient compliance
9- It can also be used as a substitute for people for whom the oral and buccal routes are unsuitable, such as those who suffer from vomiting or difficulty swallowing.

1.3.2. Disadvantages of nasal-to-brain drug delivery

Several factors reduce the drug absorption and, so, the therapeutic potency. Various challenges of nasal drug delivery to the brain are [3,6,20,21]

1- Short time available for absorption (15–30 min), due to the rapid clearance mechanism by anterior leakage, mucociliary movement, and enzymatic degradation removes the drugs from their site of absorption
2- Small administered volume 100-250 µl
3- Irritation of nasal mucosa
4- Poor permeation for hydrophilic drugs
5- Physiological changes can effect drug absorption
6- Smaller surface area in comparing with GIT
7- The molecules with weights ranging from 300 Da to 1000 Da can achieve good absorption and bioavailability; on the other hand, the molecules with the weight of 1000 Da–6000 Da are needed to be assisted by an absorbent for absorption
8- Need the design of more-complex and automated delivery devices to warrant accurate and repeatable nasal dosing
9- The prolonged contact of formulations containing cytotoxic materials can cause ciliotoxicity, and tissue damage
10- A large variance between individuals often exists for nose-to-brain drug delivery. Various factors such as head position, delivery volume, device, and method of administration can influence the absorption of formulations within the nasal cavity and the transport pathways to the brain.

1.4. Factors affecting absorption from nasal administration

To obtain relevant outcomes when performing nose-to-brain drug delivery research, the study design needs to meet certain criteria.

1.4.1. Physicochemical properties of drugs

1.4.1.1. Molecular weight

The nasal pathway provides access to larger molecules than those who get entry through the BBB, but this has its limits [22].

The molecular weight is a significant barrier to drug absorption from the nasal cavity. Nasal medication absorption is inversely correlated with drug molecular weight. The substances with molecular weights under 300 Da are readily absorbed by the aqueous nasal membrane channels [12], while; the compounds larger than 300 Da have absorption limitations. Lipophilic medicines larger than 1000 Da are absorbed less through the nose [23].

Therapeutic molecules with a molecular weight 1-6 kDa achieve good bioavailability only when permeation enhancers are used.

Figure 2 shows an inverse relationship between molecular weight and absorption of the drug [12].

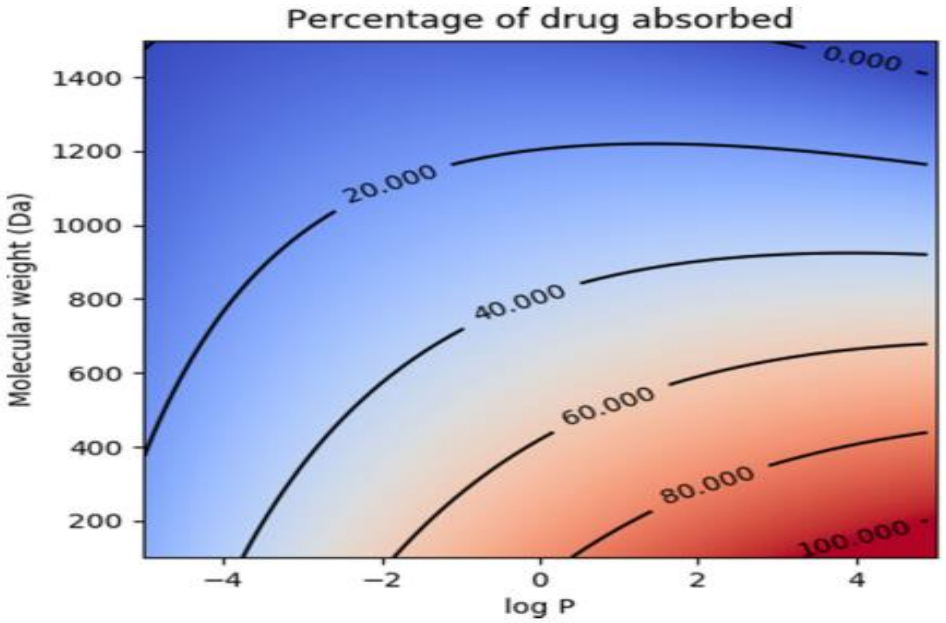

Figure 2. Percentage of drug absorbed as a function of its molecular weight and log P [(12)].

1.4.1.2. Lipophilic-Hydrophilic balance

The log P_{ow} (partition coefficient) is identified as one of the key physicochemical parameters for determining the membrane permeability of drug compounds and is written as the ratio of the concentrations of solute in the two solvents [(24)].

$$P = \frac{\{Solute\}organic\ phase}{\{Solute\}aqueous\ phase}$$

According to the partitioning coefficient theory hydrophilic and lipophilic nature of the drug will affects the process of absorption. By increasing lipophilicity, the permeation of the compound normally increases through the nasal mucosa. Although the nasal mucosa has some hydrophilic character, these membranes are mostly lipophilic in nature, and the lipid domain is crucial to their ability to act as barriers. In contrast to hydrophilic drugs, lipophilic substances are, therefore, well absorbed from the nasal mucosa [(25)].

1.4.1.3. Dissociation constant

Nonionizable and undissociated drug molecules will have a greater absorption degree in comparing with dissociated ionizable molecules, which agrees with the idea of partitioning theory because nonionizable or undissociated molecules have greater solubility in the organic phase in comparing with ionized ones [26]. The dissociation constant is affected by the drug's pKa and the pH at the absorption site (4.5-6.5 for human nasal secretion) [27].

1.4.1.4. Solubility

A drug molecule should be completely solubilized in the peri mucosal layer before being absorbed. For this, the drug molecule should be soluble in deionized water (nasal secretion is deionized watery in nature) and must have sufficient solubility that required to dissolve dose in small volume. This creates the problem for the lipophilic drugs having poor deionized water solubility. The problem can be circumvented by applying techniques aiming to enhance solubilization of bioactive by adding solubilizing agents, namely, surfactants, cosurfactants, and cosolvents, as well as by adjustment of pH, taking care of pH, pKa, nano structure, and cyclodextrins [28–30].

1.4.2. Formulation related factors affecting on absorption

A number of factors should be considered when making nasal formulations to meet requirements for efficacy and safety of nasal dosage form, including:

1.4.2.1. pH and mucosal irritation

The pH of nasal formulations should be within the physiological pH range in order to avoid nasal irritation, allow the drug to be available in a unionized form for absorption, prevent the growth of pathogenic bacteria in the nasal passage, maintain the functionality of excipients such as

preservatives, and sustain a normal physiological ciliary movement. The lysozyme is present in nasal secretions and plays a role in destroying some microorganisms at acidic pH. Nasal tissues are susceptible to microbial infection under alkaline conditions due to the inactivation of lysozyme [31,32]; it is, therefore, advisable to maintain the pH of formulations round 4.5-6.5 [27].

1.4.2.2. Osmolarity

While hypotonic formulation induces epithelial cells to expand and promote deionized water intake and drug absorption, hypertonic solutions increase cell shrinking and decrease the likelihood of release, and stimulate mucociliary clearance, which results in increased medication excretion. However, the formulation should be between 200 and 600 mOsm/l to protect the nasal mucosa's integrity since these changes might have a harmful impact during chronic treatment [12,33].

1.4.2.3. Viscosity

Nasal drug delivery has many limitations; mucociliary clearance is one of them, so a proper contact time between the drug and cell membrane is required to provide a chance for absorption, one approach that is used to increase contact time for permeation enhancement is by increasing formulation viscosity, but at another side, the viscosity should not be too high because it can effect on normal beating and clearance functions of cilia [34]. Several delivery systems are used to increase the viscosity of nasal formulations, such as gel delivery systems, in situ gel, emulgel, and mucoadhesive polymers with or without gelling agents [35–39].

1.4.2.4. Dosage form

The most prevalent and simplest nasal dosage form is nasal drops, but this dosage form is associated with rapid drainage from the absorption site.

Since solutions and suspensions do not irritate the mucosa like powder sprays, they are favored, but the powder is preferred for unstable drugs, and no preservatives or antioxidants are required form powder [34]. Recently a gel based delivery systems including in situ gel, are used to deliver a fixed dose and reduce formulation drainage to enhance residence time and drug absorption [40,41].

1.4.2.5. Pharmaceutical excipients

Every dosage form has one or more than one inactive ingredient(s) with special properties that adjust formulation properties to be compatible with the intended route of administration; in talking about the nasal environment, the excipients should be nontoxic to the nasal mucosa and cilia, nonirritant, and compatible with other composition of formula [22].

1.4.3. Physiological factors

The nasal cavity is characterized by porous epitheliums, large absorption area, rich subcutaneous blood vessels, and low enzyme activity, which makes it an advantageous administration route for rapid drug absorption and fast onset of action, with high drug permeability and avoidance of hepatic first-pass effect [42]. Several physiological factors can effect on this route including:

1.4.3.1. Mucus

The first barrier any therapy will encounter is the mucus coating which protects the nasal epithelium beneath. Mucus is a gel-like compound composed primarily of mucins which are mostly bound to membranes in mammals [43].

1.4.3.2. Mucociliary clearance

The combined defense mechanism of mucus and cilia are called mucociliary clearance, which is an essential defense against inhaled pathogens or foreign particles [44]; in normal healthy tissue, the mucociliary clearance average is about 5 mm/min, which can be altered in response to different triggers including pharmaceutical preparations [42], that lead to decrease in formulation residence time [33]. The average clearance time for an adult free from nasal disease is about 7–15 min; patients having allergy or rhinitis are likely to have accelerated mucociliary transport [45].

1.4.3.3. Enzymatic activity

Being a port to the brain, the nasal cavity has a number of enzymes present in the nasal mucosa, and on epithelial cells, these odorant-metabolizing enzymes (OMEs) are a member of xenobiotic-metabolizing enzymes (XMEs) [46]; the research in this field confirmed that nasal tissue is an effective toxicological barrier, but the pattern of enzyme expression in the olfactory endothelium is quite different from that in the liver, the olfactory endothelium presents a large network of XMEs [47].

1.5. Overcoming barriers in nasal drug delivery

Even while nasal administration of a large variety of pharmaceuticals is effective for CNS and systemic delivery, some medications nevertheless have low bioavailability.

The low bioavailability may be due to the limited drug solubility, quick enzymatic breakdown in the nasal cavity, poor membrane permeability, and quick mucociliary clearance could all contribute to low bioavailability.

Several methods that mimic preferred conditions for the nose-to-brain route are available, with the aim to enhance brain uptake by increasing the

permeability, prolonging the retention time on the nasal epithelium and, therefore also on the olfactory region, and increasing bioavailability [48]. These barriers can be overcome by : [34]

1.5.1. Prodrug approach

Some disadvantages of nasal drug delivery system from the unique architecture of the nasal cavity; most of the problems are due to the inherently unfavorable physicochemical properties of the drug molecule. Hence, it is possible to achieve optimal absorption by the nasal route of administration by chemical derivatization of the drug molecules [49].

The rationale behind the utilization of the prodrug approach is for the enhancement of drug aqueous solubility and passing nasal enzymatic activity for unstable drugs [31].

1.5.2. Solubilizing agents

It is challenging to develop medications that have low deionized water solubility at high strengths without including a lot of cosolvents or surfactants, which are potentially harmful excipients. This is an even bigger issue with nasal delivery since, as was previously indicated, the drug must be supplied in a small volume, necessitating even higher drug strengths [32,50].

A large number of solubilizing agents that used nasally, such as cyclodextrin derivatives, cosolvents, and surfactants [51].

1.5.3. Enzyme inhibitors

Although intranasally delivered drugs are by passed liver metabolizing effect, they will face some enzymes in the nasal lumen, but these enzymes have different expressions from liver enzymes, and they do not have a significant effect on the extent of absorption of most of the compounds except protein and peptide molecules [47].

Particularly, enzyme inhibitors such as bestatin, amastatin, boroleucin, borovaline, aprotinin, and trypsin inhibitors are essential components of the

formulation while developing a dosage form for protein and peptide molecules [22].

1.5.4. Absorption enhancers

To enhance the bioavailability and absorption of high molecular weight compounds (such as peptides and proteins), nasal permeation enhancers are to be used widely.

Absorption enhancer agents are well explored for the nasal drug delivery system, and the most commonly explored agents are surfactants, bile salts, fatty acids (taurodihydrofusidate), and polymeric enhancers (chitosan, cyclodextrins, poly-L-arginine, and aminated gelatin) [28].

1.5.5. Mucoadhesive agents

A significant drawback of nasal delivery is that mucociliary clearance shortens the time that a formulation is in touch with the nasal mucosa, which can be improved by the use of mucoadhesive agents as a vehicle of the drug to allow sufficient time for the drug to activate its therapeutic effect [52].

Mucoadhesion includes an interaction of the mucoadhesive polymer with mucin, mucoadhesive natural or synthetic polymer such as Chitosan, Hypromellose, Carbopol®, Carboxymethylcellulose, Polyacrylic acid or others have been extensively used as excipients for nasal formulations, and most mucoadhesive molecules are positively charged to build-up interactions with the negatively charged mucins on the apical surface of epithelial cells. Mucoadhesion involves two steps: a contact stage followed by a consolidation stage. In the contact stage, wetting and swelling occur in the mucoadhesive formulation when the polymer spreads over the mucus membrane to develop a deep contact with the mucus layer. Subsequently, the consolidation stage involves physicochemical interactions that establish and consolidate the adhesive interaction. In this stage, the mucin chains entangle with the mucoadhesive polymer chains, resulting in mechanical bond

formation. Then, moisture's presence promotes the formation of chemical bonds such as hydrogen bonds, covalent bonds, and weak van der Waals forces that strengthen the system [53].

1.5.6. Nanocarrier formulations

The tight junction of nasal epithelium and enzymatic metabolism of the drug is responsible for reducing the effectiveness of the nasal route of delivery to the CNS. The strategy of encapsulating drugs into the nanocarriers could significantly improve the delivery to the brain via the nasal route, such as nanoparticles, lipid-based nanoparticles, liposomes, microemulsion, microspheres, and nanogel [54,55].

1.5.7. In-Situ gel delivery system

In situ gel can be used in ophthalmic administration, nasal administration, rectal administration, and vaginal administration [37].

The most significant issues that persist with nasal solutions are quickly eliminated from the nasal cavity. For liquid and powder formulations that are not mucoadhesive, the clearance half-life is in the range of 15 to 30 minutes. In addition to the mucoadhesive approach mentioned above, utilizing viscosity-enhancing or in situ gelling polymers to extend the contact period with the nasal surface. An intelligent drug delivery system responding mainly to physiological stimuli has emerged as an innovative approach for the delivery of therapeutic agents. Owing to their properties, in situ gelling formulations have the ability to undergo a phase transition, a solution to gel formation, triggered by physiological factors upon nasal administration (e.g., temperature, ion concentration, pH). In situ gel provide a number of advantages over conventional gels, including the ability to be delivered accurately and consistently, the ability to be easily injected in liquid form,

and the ability to extend the residence period of the formulation on the surface of the nasal cavity due to gelling [42].

Systems for in-situ gelling fall into three categories: ion-activated systems (e.g., gellan gum and sodium alginate), temperature-dependent systems (e.g., Pluronic, Tetronic, and polymethacrylates), and pH-triggered systems (e.g., Carbopol and cellulose acetate phthalate) [18].

The mechanism of phase transition is based on a marked change in the aqueous solubility of polymers that are characterized by the presence in their structure of hydrophobic and hydrophilic groups. Formulation scientists can manipulate the concentration of stimuli-responsive in situ gelling polymers to control the rate and extent of gel formation, residence time, and drug release rate without requiring additional organic solvents or co-polymerization agents to trigger gel formation [74].

The triggering mechanism responsible for the phase transition of the stimuli-responsive in situ gels is divided into two major categories; the first is physical crosslinking (pH, temperature, ionic change), and the second is chemical crosslinking (magnetic field, light, electrical signal). Usually, owing to the ease of fabrication and safety profile, physical crosslinking is preferred over chemical crosslinking for in situ gelations. It is a conventional method of in situ gelations that involves the use of temperature, ionic and pH modulation as triggering factors [61].

1.5.7.1. Physical approaches for Inducing In-Situ Gelling System

I- Thermo-responsive in situ gel

The concept involves the development of formulations comprising polymers that exhibit temperature-triggered sol-to-gel transitions in the range of room temperature–37°C.

The commonly used polymers can be broadly classified into synthetic polymers, including poloxamers and poly(N-isopropylacrylamide) and natural polymers cellulose derivatives.

A commonly used synthetic polymer is Poloxamer 407 (PoloX407), which is known to bear thermosensitive properties.

Natural and synthetic derivatives from natural sources polymers, including xyloglucan, mucilage gel extract from F. Carica, and trimethyl chitosan, show thermosensitive dependent sol-to-gel transitions [62].

These polymers are categorized into two classes; first, polymers that become insoluble above a critical temperature called the lower critical solution temperature (LCST), and second, polymers that precipitate and undergo phase change below a critical temperature called the upper critical solution temperature (UCST) (Figure 3). LCST polymers are called "negative temperature–sensitive polymers," for example poloxamers.

UCST polymers are referred to as "positive temperature–sensitive polymers"; for example, poly(acrylic acid) (PAA), polyacrylamide (PAAm), and poly(acrylamide-co-butyl methacrylate) [63].

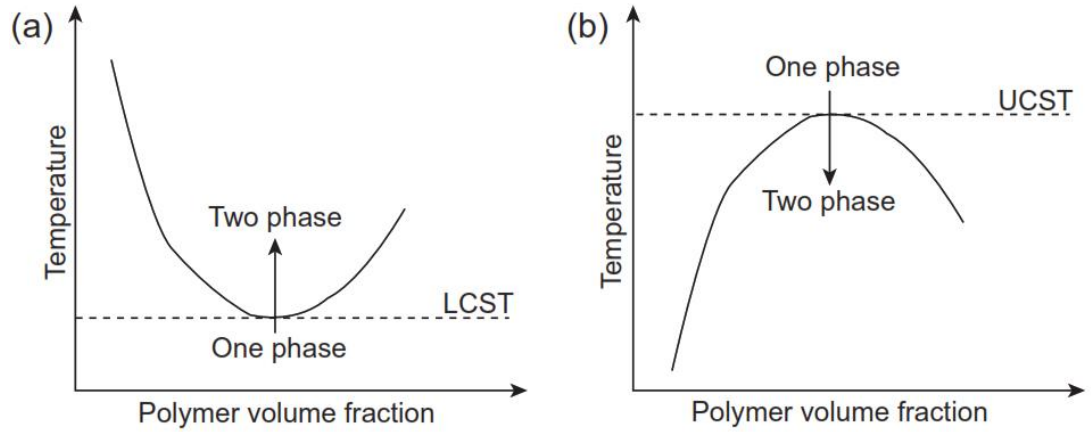

Figure 3. Phase transition phenomenon. (a) Lower critical solution temperature (LCST) and (b) upper critical solution temperature (UCST) phase transition behaviors of thermo-responsive polymers in solution [63].

II- Ion responsive in situ gel

It is well-known that some anionic polysaccharides (alginate, gellan gum, and pectin) are ion-sensitive polymers; they are cross-linked by some

monovalent (Na^+) and/or divalent (Mg^{2+} and Ca^{2+}) cations present in different physiological fluids [18].

III- pH responsive in situ gel

Polymers containing acidic or alkaline functional groups that respond to changes in pH are called pH sensitive polymers [59].

Most of the pH sensitive polymers containing the anionic group are based on polyacrylic acid (Carbopol®, Carbomer) and its derivatives that form a gel when pH value increase from acidic to neutral. Other polymers which show pH induced gelation are cellulose acetate phthalate latex, poly methacrylic acid, polyethylene glycol, and pseudo latexes [64].

The swelling of hydrogel increases as the external pH increases in the case of weakly acidic (anionic) groups but decreases if the polymer contains weakly basic (cationic) groups [65].

1.5.7.2. Advantages of in situ gel system

Overcoming the drawbacks associated with conventional drug delivery systems and taking advantage of both solutions and gels, such as [66]:

1- Accurate dosing
2- Ease of administration
3- Longer residence time
4- Provides more bioavailability
5- Decreases the wastage of drug
6- Reduces the frequency of administration
7- Allows patient compliance and comfort
8- Administered to unconscious and old patients
9- Doesn't permit drug accumulation (due to low dose)
10- Exhibits bio-adhesiveness to facilitate drug targeting.

1.5.7.3. Ideal properties of Thermo-sensitive Nasal In-Situ Gel

1- Sol-to-Gel gelation time and temperature

The critical parameters that must be estimated to optimize thermosensitive gel are the gelation temperature and gelation time.

An excellent thermo-responsive in situ gel typically achieves sol-gel transition at the physiological temperature of the nasal cavity and has a glass transition temperature above room temperature. Hence, it is preferred that nasal in situ formulations have a gelation temperature above room temperature and below 35°C [(37)].

Gelation time is the length of time needed for the start of gelation and the subsequent change from sol to gel. Both gelation temperature and gelation time depend on the concentration of thermosensitive polymer(s) as well as on other additives. In general, when the concentration of thermosensitive polymer increased, more micelles formed, which decreased the gelation time and temperature [(78)].

2- Rheological properties

The viscosity of a thermosensitive in-situ gel formulation changes directly in response to temperature change. The nasal clearance of given formulations is slowed down by the conversion of polymer-based liquid formulations into gels as a result of rising temperature. It should be of low viscosity before instillation. The flow of nasal in situ gel (sol) should be free to allow reproducible administration to the nasal cavity, as a spray or as a droplet mist [(20)].

3- Mucoadhesive properties

In order to provide mucoadhesion and hence increase residence at the application site, mucoadhesive polymers are typically used in nasal in situ gel formulations [(67)].

1.5.7.4. Properties of the polymers used for thermosensitive In-situ gelling

The polymers used for in situ gel formation should have the following properties [68,69]:

1- It should be biocompatible and non-immunogenic; it should not provide any toxic effects and should be biodegradable.

2- It should have a suitable critical solution temperature, and these polymers can be modified to show sol-gel transition at the desired temperature.

3- It should improve mechanical properties.

4- It should provide a stable formulation at storge conditions.

1.6. Nasal thermosensitive mucoadhesive polymers

Polymeric materials are widely used in a broad range of pharmaceutical products and constitute essential components of modern dosage forms. Therefore, it is important to understand polymer properties in order to enable the rational design and development of drug delivery systems.

1.6.1. Poloxamer

The word ‘poloxamer’ was coined by the inventor Irving Schmolka, who received the patent for these materials in 1973.

Poloxamers are examples of LCGT biocompatible thermoreversible gels that were introduced in the 1950s by BASF (Iselin, NJ, USA). Poloxamers are triblock copolymers, available under the trade name of Pluronic®(BASF), Lutrol®(BASF), Kolliphor® (BASF), Synperonic® (Croda), and Antarox® (Rhodia) [70].

Poloxamers are FDA approved and listed as excipients in the U.S. and British pharmacopeias; they are non-toxic and non-irritant [71].

Poloxamers or Pluronic ® are a class of deionized water-soluble nonionic triblock copolymers formed by polar (poly ethylene oxide) (PEO) and non-polar (poly propylene oxide) (PPO) blocks, which confer amphiphilic and surface-active properties to the polymers. Their aqueous solutions undergo sol-to-gel transition with increasing the temperature above an LCGT [71].

1.6.1.1. Poloxamer 407 (PoloX 407)

Among the poloxamers, Poloxamer 407, with registered trademarks of Pluronic® F127 by BASF Laboratories and Synperonic PE/F127® by ICP Laboratories, is a non-ionic surfactant with a wide range of applications. Poloxamer 407 is known as an "inactive ingredient" by U.S. Food and Drug Administration (FDA) for a variety of drug products such as oral solutions, suspensions, inhalation formulations, intravenous (I.V), ophthalmic or topical formulations [72].

Poloxamer 407 is a copolymer with a molecular weight of around 12.6 kDa (POE101 POP56 POE101), and it has a polyoxyethylene content of about 70%, which adds to its hydrophilicity. Its chemical structure is shown in Figure 4 [73]. It is a non-ionic surfactant that is compatible with cells, body fluids, and a variety of substances, in addition to having excellent solubilizing capacity, low toxicity, and good drug release qualities [74].

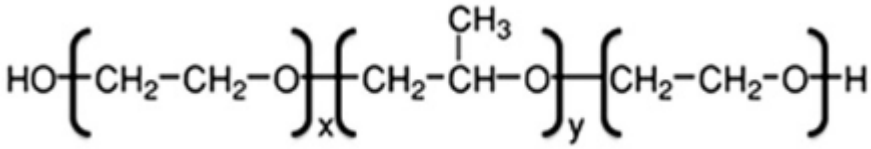

Figure 4. Chemical structure of poloxamer 407 [73].

Poloxamer 407 is often used in association with other poloxamers, especially poloxamer 188, in order to modulate the $T_{sol\text{-}gel}$ [74].

1.6.1.2. Poloxamer 188 (PoloX 188)

Poloxamer 188 (Pluronic F-68, Flocork), in its entirety, is a mixture of nonionic macromolecules. Each molecule consists of a central polypropylene oxide chain flanked at either end by a polyethylene oxide segment, thus forming an ABA block copolymer structure [75].

Although they have the same chemical structure as other poloxamers, what differs among them is their molecular weight due to the variation in the quantity of poly (propylene oxide) and poly (ethylene oxide) units [68].

Poloxamer 188 is known to have low toxicity, excellent deionized water-solubility, high solubilizing capacity, good drug release characteristics, compatibility with other chemicals, and cause less skin irritation [76]. Figure 5 shows the chemical structure of poloxamer 188.

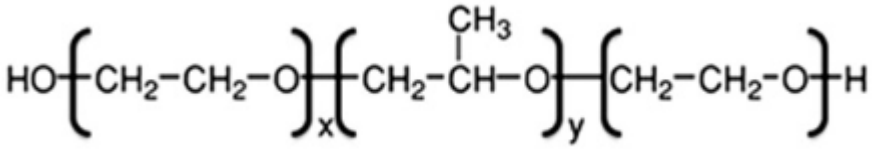

Figure 5. Chemical structure of poloxamer 188 [73].

1.6.2. Mucoadhesive polymers

The choice of excipients and polymers that provide adhesion to the mucous membrane should be based on specific indicators, including the effect on the critical gelation concentration, optimal pH, and rheological properties.

Hydroxypropyl methylcellulose (HPMC); or may be called Hypromellose; methyl hydroxypropyl cellulose; propylene glycol ether of methylcellulose; or methyl cellulose propylene glycol ether, 2-hydroxypropyl methyl ether, cellulose hydroxypropyl methyl ether. It has the chemical formula of $C_8H_{15}O_6$-($C_{10}H_{18}O_6$)-$C_8H_{15}O_5$.

Hydroxypropyl methylcellulose (HPMC) belongs to the group of cellulose ethers in which hydroxyl groups have been substituted with one or more of the three hydroxyl groups present in the cellulose ring (Figure 6) [77].

HPMC is hydrophilic (deionized water soluble), a biodegradable, and biocompatible polymer having a wide range of applications in drug delivery [78].

The HPMC is a white, yellowish-white, or greyish-white powder or granules, hygroscopic after drying; it is practically insoluble in hot deionized water, in acetone, in anhydrous ethanol, and in toluene. It dissolves in cold deionized water, giving a colloidal solution [79].

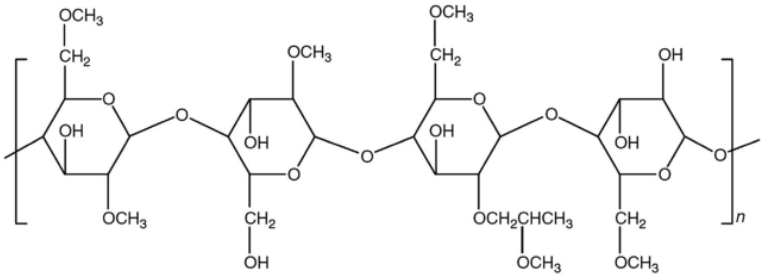

Figure 6. Chemical structure of HPMC [73].

Hyaluronic acid (HA) (also known as sodium hyaluronate or hyaluronan) is a straight-chain, natural polysaccharide, and the basic structure consists of two repeating saccharide units, namely D-glucuronic acid and *N*-acetyl glucosamine. Figure 7 shows the chemical structure of hyaluronic acid [80,81].

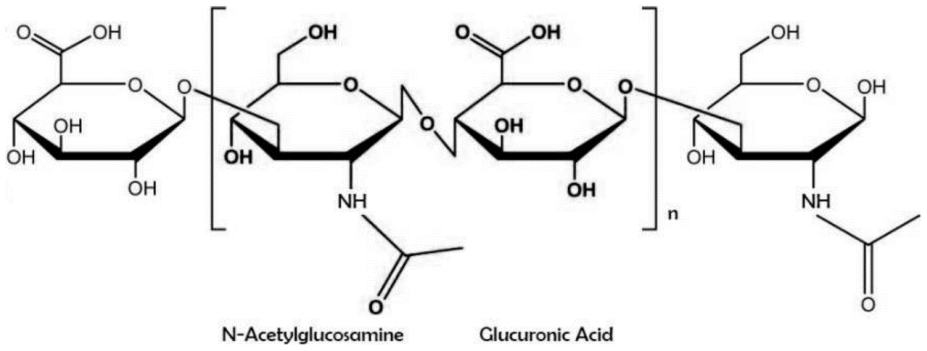

Figure 7. Chemical structure of hyaluronic acid with repeating disaccharide units [73].

Owing to its biocompatibility and biodegradability, HA and its derivatives have been described as valid mucoadhesive with excellent biocompatibility and biodegradability [82].

It has been proposed that the main force responsible for mucoadhesive properties of HA is the formation of hydrogen bonds between the hydrophilic carboxyl and hydroxyl groups and the mucus components [83].

According to the European Pharmacopoeia, Carbopol® (Car934) by chemical structure are the polymers of acrylic acid, cross-linked polyalkyl esters of sugars or polyalcohols. Figure 8 shows the chemical structure of Carbopol [77].

This polymer contains from 56.0 to 68.0% of carboxyl (-COOH) groups calculated with reference to the dried substance. Carbomers do not dissolve in deionized water but only swell, forming during hydration and neutralization colloidal dispersions characterized by apparent viscosity [84].

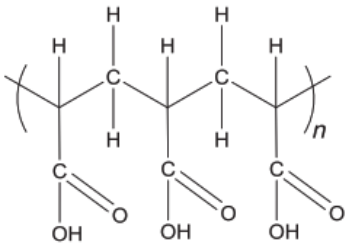

Figure 8. Chemical structure of Carbopol [73].

Methylcellulose (MC) is a methyl ester of cellulose (Figure 9) [85] that contains 27.5- 31.5% of the methoxy groups. MC is soluble in deionized water, and its aqueous solution exhibits thermal gelation properties [77].

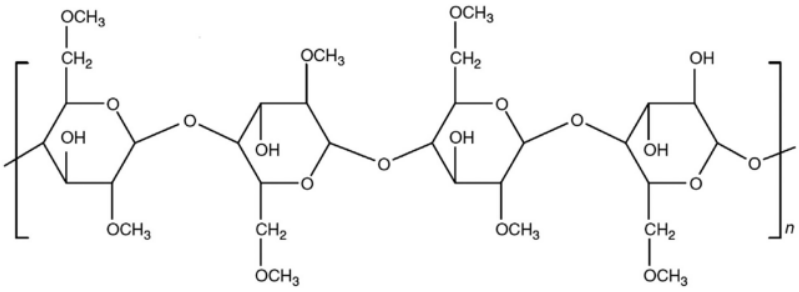

Figure 9. Chemical structure of methylcellulose [73].

1.7. Nefopam HCl (NF)

1.7.1. Definition

In the early 1970s, nefopam was developed as an antidepressant and was also used as a myorelaxant for the treatment of spasticity. The additional analgesic property was soon recognized [86].

1.7.2. Pharmacological effect

Nefopam a benzoxazocine an orphenadrine derivative, is a centrally acting non-opioid analgesic with both supraspinal and spinal sites of action. It inhibits the reuptake of serotonin, dopamine, and noradrenaline and is neither an opiate nor a non-steroidal anti-inflammatory drug. It does not cause respiratory depression [87].

1.7.3. Physicochemical properties

Chemically, Nefopam Hydrochloride is 5-methyl-1-phenyl-1,3,4,6 tetrahydro-2,5-benzoxazocine;hydrochloride, $C_{17}H_{19}NO.ClH$, (Figure 10) and its molecular mass 289.8, log P 3.4, pKa 8.98, and its melting point is 260 ˚C, registered in European Medicines Agency (EMA) and European Chemicals Agency (ECHA) [88].

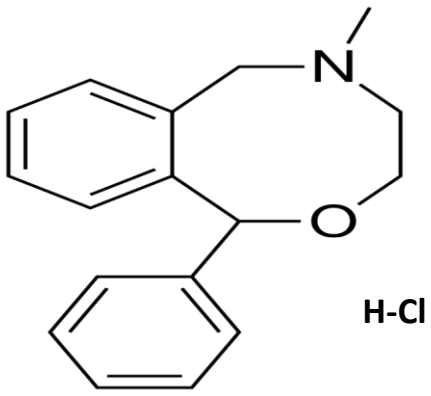

Figure 10. Chemical structure of Nefopam Hydrochloride [88].

Nefopam Hydrochloride has been classified as class I according to Biopharmaceutical Drug Disposition Classification System (BDDCS) (Class I have high solubility and extensive metabolism) and Biopharmaceutical Classification System (BCS) (Class I have high solubility and high permeability) [89].

1.7.4. Dose

Nefopam HCl marketed as a coated tablet, and ampoule for intramuscular and intravenous used for relief of moderate acute and chronic pain. The usual oral dose range is 30 to 90 mg three times daily. Nefopam hydrochloride may also be given in doses of 20 mg by intramuscular injection, repeated every 6 hours if necessary; It has also been given by slow intravenous injection in doses of 20 mg every 4 hours up to a maximum of 120 mg daily [89].

1.7.5. Pharmacokinetic properties

Nefopam HCl is absorbed from the gastro-intestinal tract. Peak plasma concentrations occur about 1-3 hours after oral administration. About 73% is bound to plasma proteins. It has an elimination half-life of about 4 hours.

It has a limited bioavailability (approximately 36%) as a result of liver first-pass hepatic metabolism. Three of seven water-soluble metabolites are reported in humans; N-desmethyl nefopam, nefopam-N-oxide, and its N-glucuronide; are mostly excreted in the urine.

Nefopam HCl is excreted mainly in the urine. Less than 5% of a dose is excreted unchanged in the urine. About 8% of a dose is excreted via feces [89].

1.7.6. Side effects

The undesirable side effects of NF mainly due to systemic anticholinergic activity including blurred vision, palpitations, tachycardia, hypotension, dry mouth, gastrointestinal disturbances, urinary retention [90].

1.8. Literature review

Several studies have formulated nefopam for improving bioavailability and reducing side effects.

Only one study has developed nasal delivery systems of nefopam; Heba Abou-Taleb et al. formulated nasal niosomes loaded with nefopam with improved bioavailability [91]; in addition to the conventional route of administration mentioned above, nefopam formulated as transdermal matrix patch system by Pintu De et al. [92], Nefopam hydrochloride loaded microspheres, was developed by S. Sukhbir et al. and Neelam Sharma et al. [93–95], M. El-Mahdy developed Nefopam hydrochloride microcapsules [96], Uphade K. B. Et al. formulated Osmotic Tablet of Nefopam Hydrochloride [97].

Aim of the study

The aim of this work was to formulate and optimize a thermosensitive nasal mucoadhesive in situ gel of nefopam hydrochloride as atrial to enhance its brain-targeting.

Chapter Two Experimental work

2. Experimental work

2.1. Materials

A list of materials and reagents that were used in this study with their suppliers is shown in Table 1.

Table 1. Materials and Reagents Used in the Study.

Materials and Reagents	Manufacturer company
Benzalkonium chloride	Shanghai UCHEM Inc., China
Hydrous Calcium chloride ($CaCl_2.2H_2O$)	Baoji Guokang Bio-Technology Co., Ltd, China
Carbopol ® 934	Eastman Chemical company, United states of America
Hyaluronic acid	Baoji Guokang Bio-Technology Co., Ltd, China
Hydroxypropyl methylcelluloseK4M (HPMC K4M)	Eastman Chemical company, United states of America
Nefopam Hydrochloride	Baoji Guokang Bio-Technology Co., Ltd, China
Poloxamer 188	Eastman Chemical company, United states of America
Poloxamer 407	
Potassium chloride (KCl)	Baoji Guokang Bio-Technology Co., Ltd, China
Sodium chloride (NaCl)	

2.2. Instruments

A list of instruments that were used in this study with their manufacturer is shown in Table 2.

Table 2. Instruments Used in the Study.

Instruments	Supplier Company
Centrifuge	Hettich, Germany
Differential scanning calorimeter	Shimadzu 60 Plus
Electronic analytical balance	Kern, Germany
Fourier transform infrared spectrometer	Lambda 7600, Australia Shimadzu, Japan
Franz diffusion apparatus	Copley, England
Humidity Oven	Gallenhamp, England
Magnetic stirrer	Stuart, England
Melting point apparatus	Stuart, England
Osmometer (OSMOMATO 030)	Gonotec, Germany
pH meter HI98107	Hanna, Italy
UV-Vis. spectrophotometer	Varian Cary 100 bio, Australia
Viscometer	Myr VR 3000, Spain
Deionized water bath	BS-11, Jeio Tech, Korea Thermostat water bathHH-1, China

2.3. Method

2.3.1. Characterization of NF

2.3.1.1. Measurement of melting point

An open capillary tube method was used to determine the melting point, as stated by the USP. It used a capillary glass tube that was sealed by one side; the other open side of the capillary tube was dipped in the powder of Nefopam hydrochloride (NF) and subsequently tapped smoothly on the solid surface. Then, at room temperature, the capillary tube was put into the electrical melting point apparatus, then the temperature was increased gradually and observed until the drug melted. The melting point range was recorded from starting of the melt till the end of the melt [98].

2.3.1.2. Differential Scanning Calorimetry (DSC)

DSC is a thermal analytical method in which the alteration in the quantity of heat is essential for raising the temperature of a sample. A small quantity of NF was sealed in ordinary aluminum pans and then heated at a rate of 10°C every min. over a range of temperatures 50°C to 300°C [99].

2.3.1.3. Determination of λ_{max} of NF

A stock solution of NF (1 mg/mL) was prepared in deionized water, simulated nasal fluid (SNF, NaCl 7.45 g/L, KCl 1.29 g/L, and $CaCl_2.2\ H_2O$ 0.32 g/L.)(150), and Aqueous phosphate buffer saline (pH 7.4).

UV-VIS spectra scan 200-400 nm were recorded after a suitable dilution.

2.3.1.4. Construction of calibration curves of NF

The calibration curves of NF in deionized water, SNF, and aqueous phosphate buffer saline was prepared through a series of dilutions at various concentrations (50-300) μg/ml from the stock solution (1 mg/ml). The

absorbance was measured at λ max of the NF. The measured absorbance was plotted against the respective concentration [100].

2.3.1.5.Determination of NF saturated solubility

The test tube method measures the solubility of drugs in an aqueous buffer, simulated nasal fluid, and deionized water by adding an excess amount of NF in 10 ml of solvents mentioned above in a glass tube, then stored at 34°C in a shaker water bath for 72 hours to reach an equilibrium state. After that, a solution is centrifuged at 3000 rpm for 15 min; then, the solution was filtered using 0.45 μm filter paper and a final concentration of NF is measured after a suitable dilution to be read by UV-VIS [101]. This test was checked in a triplicate manner.

2.3.2. Formulation of poloxamer dispersion

The cold method has been used to formulate different compositions of thermosensitive in situ gel, as detailed in Table 3, by blending different concentrations of Poloxamer 407 (PoloX 407) (17-20%) with or without Poloxamer 188 (PoloX 188) (3-4%) in cold deionized water immersed in ice with continuous stirring for 4-6 hours, the dissolution of the polymer takes place under continuous and slow stirring in order to avoid the formation of foam. Then the obtained cloudy mixture was stored in the refrigerator at 4°C for 24 hours to get a clear solution. the gelation temperature was determined for each formula; only compositions with a gelation temperature range of 30-36°C [102] were selected for further addition to the final formula.

Table 3. Compositions of Nasal In-Situ Gel Polymer Mixture (P).

P No.	PoloX 407 (%w/v)	PoloX 188 (%w/v)	D.D.W q.s ml
1	17		10
2	18		10
3	19		10
4	20		10
5	17	4	10
6	18	4	10
7	19	4	10
8	20	4	10
9	17	3	10
10	18	3	10
11	19	3	10
12	20	3	10

2.3.2.1.Preparation of thermosensitive mucoadhesive in situ gel

The cold method was used to prepare thermosensitive mucoadhesive NF in-situ gel formulas; the solubilization of the poloxamer in the aqueous phase is the starting point as mentioned above, and the addition of the mucoadhesive polymer was according to the type of mucoadhesive polymer properties and solubility in poloxamer solution.

The mucoadhesive polymers HPMC K4M, Car934, HA, and MC, were added to poloxamer dispersion in different concentrations, as shown in Table 4; the addition of the polymer was slowly and gradually at 4°C to a selected poloxamer mixture with continuous stirring for 30 min at slow rpm about (50 rpm) to prevent foam formation.

Cold procedures result in a transparent, colorless and clear liquid dispersion.

Then NF and Benzalkonium chloride (BNZ) at a concentration (20 mg/ml) and (0.01 % w/v), respectively, were added slowly with continuous slow stirring to prevent foam formation, and complete the volume with deionized water up to 10 ml.

Finally, the mixture was stored for 24 hours at 4 ºC to eliminate a formed foam.

Table 4. Compositions of the Formulated Nasal In-Situ Gel with Mucoadhesive Polymers

F. No.	NF mg	PoloX 407(%)	PoloX 188(%)	HPMC K4M (%)	HA (%)	Car934 (%)	MC (%)
1	200	17		1			
2	200	19	4	1			
3	200	18	3	1			
4	200	19	3	1			
5	200	17		0.75			
6	200	19	4	0.75			
7	200	18	3	0.75			
8	200	19	3	0.75			
9	200	17		0.5			
10	200	19	4	0.5			
11	200	18	3	0.5			
12	200	19	3	0.5			
13	200	17			0.75		
14	200	19	4		0.75		
15	200	18	3		0.75		
16	200	19	3		0.75		

F. No.	NF mg	PoloX 407(%)	PoloX 188(%)	HPMC K4M (%)	HA (%)	Car934 (%)	MC (%)
17	200	17			0.5		
18	200	19	4		0.5		
19	200	18	3		0.5		
20	200	19	3		0.5		
21	200	17			0.25		
22	200	19	4		0.25		
23	200	18	3		0.25		
24	200	19	3		0.25		
25	200	17				0.3	
26	200	19	4			0.3	
27	200	18	3			0.3	
28	200	19	3			0.3	
29	200	17				0.2	
30	200	19	4			0.2	
31	200	18	3			0.2	
32	200	19	3			0.2	
33	200	17				0.1	
34	200	19	4			0.1	
35	200	18	3			0.1	
36	200	19	3			0.1	
37	200	17					0.3
38	200	19	4				0.3
39	200	18	3				0.3
40	200	19	3				0.3
41	200	17					0.2
42	200	19	4				0.2

F. No.	NF mg	PoloX 407(%)	PoloX 188(%)	HPMC K4M (%)	HA (%)	Car934 (%)	MC (%)
43	200	18	3				0.2
44	200	19	3				0.2
45	200	17					0.1
46	200	19	4				0.1
47	200	18	3				0.1
48	200	19	3				0.1

2.3.3. Characterization of NF Nasal in situ Formulas

2.3.3.1. Gelation temperature

Each glass tube that contained 2 ml of the formulation was kept in the at 25ºC; then, the temperature raised gradually at a rate of 1ºC / min, and at the end of the minute, a glass tube titled at 90 ^{0} in a horizontal position, as shown in Figure 11 to show if the solution is converted into a gel, gelation temperature was recorded when no movement of solution occurred as a result of conversion into a gel, this test is checked in a triplicate manner [(103)].

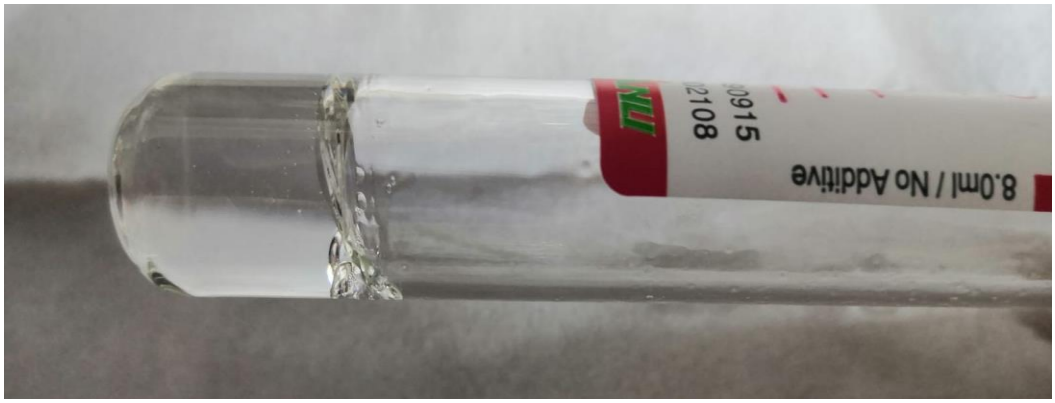

Figure 11. Gel formation triggered by temperature

This test is the governing test, the concentration of the best combination of poloxamer and also the best concentration of the mucoadhesive polymer were chosen from this test.

2.3.3.2. Clarity and appearance visualization

Visual inspection of nasal in-situ formulas was performed for all the 48 formulas against the white and black paper in triplicate were conducted to examine the occurrence of any incompatibility due to an interaction between active pharmaceutical ingredient (API) with excipients or among excipients themselves. A change in color or precipitation was considered a sign of incompatibility [104], and the formulas that passed this test were used for further evaluation.

2.3.3.3. Gelling time and capacity determination

The gelling capacity was determined by adding 1 mL of the system to a vial containing 2 ml of freshly prepared and equilibrated at 34° C simulated nasal fluid, visually observing the gel formation and noting the time for gelation every 5 sec for 1 minute or till gel formation. and noting the time taken for the gel formed to dissolve, every 15 min. The gelling capacity was determined in triplicate [105].

2.3.3.4. pH measurement

The pH of the selected formulas were measured by using pH meter, in triplicate at room temperature. Initially, pH 4 and pH 7 standard buffer solutions were utilized to calibrate the equipment, then pH meter probe dipped inside the formulations to record its pH values [106].

2.3.3.5. Drug content test

Accurately, 1 mL of the formulation (equivalent to 20 mg/mL NF) from selected formulas were diluted to 10 mL with SNF A 1 mL of this diluted solution was diluted again to 10 mL with SNF Then the solution was filtered by a 0.45 μm syringe filter. Finally, the absorbance was measured at the maximum absorption wavelength using a UV-VIS spectrophotometer.

The samples were taken from three different regions of the gel the upper, middle, and bottom of the formulas to ensure uniform distribution of NF in solution, and the mean drug content was measured [107].

2.3.3.6. Osmolarity measurement

Osmotic pressure was measured by using the osmometer, that was zeroed by purified deionized water and then 300 mOsmol NaCl (1%NaCl) standard solution for calibration. Then, 50 µL of the formulas were used in a clean, dry microtube. After checking for bubbles of air, the measurement was performed [108]. and the results were recorded in triplicate.

2.3.3.7. Gel strength measurement

Gel strength was measured in triplicate by weighing 5 g of formulas were placed in a 10 mL measuring cylinder using a temperature-controlled deionized water bath; they congealed at 34°C. A 3.5 g of weight was applied pressure on the gel through a circle cup. The time (sec.) taken by weight of 3.5 g to penetrate 0.5 cm through the gel was recorded [106]. As shown in Figure 12**.**

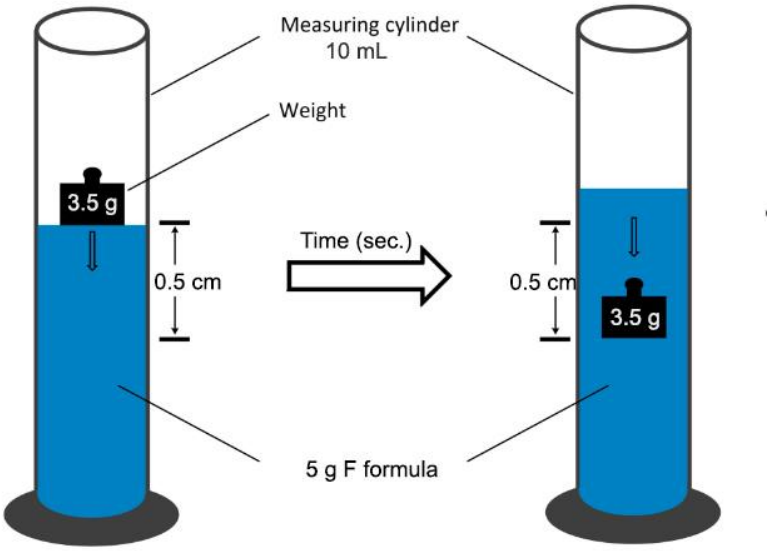

Figure 12. Gel strength test scheme

2.3.3.8.Spreadability Test

The spreadability of the formulas was measured by spreading 0.5 g of the gel on a circle of 2 cm diameter premarked on a glass plate, and then a second glass plate was employed. 0.5 kilogram of weight was permitted to rest on the upper glass plate for 5 min. The total diameter of the circle after spreading the gel was determined in (cm) [109].

2.3.3.9.Mucoadhesive strength measurement

The detachment force resulted from utilizing a modified pan balance to measure the force necessary to separate the gel from sheep nasal mucosal tissue for formulas as shown in Figure 13. A sheep nasal mucosa was obtained from the slaughterhouse. The sheep's nasal mucosa was delicately removed from its nasal cavity and preserved in a simple saline solution. It was prepared for usage after blood and bone cartilage were taken out of the mucosal membrane. The mucosal side was stored in a glass vial. They were kept at 34°C for 5 min before securing them to the device. On one side, a modified vial was positioned in an inverted manner and held 1 mL of formula, while the other side held a small plastic beaker that had been weighted previously. The establishment of intimate contact between tissue fixed on a petri dish under the vial and the formula was confirmed by allowing a 2-minute contact duration. On the opposite side, the plastic pan's weight increased until a detachment of gel from the tissue occurred. The minimum weight needed for tissues to separate from the surface for each formulation, detachment stress calculated using the equation:

$$\textit{Detachment stress (dynes/cm}^2\textit{)} = M * G / A \qquad \textbf{\textit{Eq 1.}}$$

where M = Minimal weight required for separation of two vials in g, G = Gravitational acceleration (980 cm/s^2) and A = exposed tissue area. For each measurement, the newly formed nasal mucosa was employed [106].

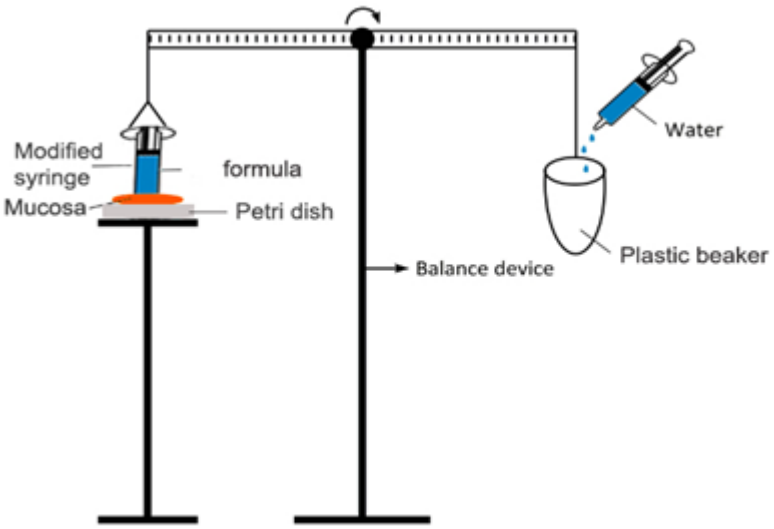

Figure 13. Mucoadhesive strength test scheme

2.3.3.10. Rheological studies

The rheological properties of (F 13 - 45) were evaluated by the viscometer, that is initially calibrated after being balanced on the surface.

The samples' viscosities were measured at room temperature for the solution phase and at 34 °C for the gel phase in triplicates. Samples were sheared at 10 rpm with spindle R4 and R5 for a solution and at 10,12, 20, 30,50,60,100,200 rpm with spindle number R7 for gel [106].

Plots of shear rate (rpm) versus viscosity (cP) were used to establish the interpretation of rheological behavior.

2.3.3.11. *In-vitro* drug release study

The modified Franz diffusion cell was used to perform a drug release study. The experiments performed at 34°C with a continuous stirring of 50 rpm, using a magnetic bead, for 2 hours. Simulated nasal fluid (SNF) as the receptor medium. A dialysis membrane, having a molecular weight of 12000-14000 Dalton and pore size 2.5 nanometers, was immersed in SNF for 2 h before use. Enough SNF (15 ml) to achieve a sink condition was placed in the receptor compartment. 1 mL of formulas that contain 20 mg of

NF were taken in the donor compartment, and the temperature was increased to 34°C to allow the formation of a gel. 2 mL of receptor fluid was taken out at the designated time (every 5 min.), and fresh receptor fluid was substituted to keep the sink condition. By using spectrophotometry, the amount of NF that diffused through the dialysis membrane was calculated at lambda max using UV-Vis after diluting suitably with SNF [110].

The control drug release was performed with the same procedure mentioned above, with the use of 20 mg NF aqueous solution without any additives, to compare the drug release from selected formulas and free drug.

2.3.3.11.1. Analysis of release mechanism

The mechanism of NF release from different formulas were mathematically analyzed according to different mathematical release equations, including:

1- **Zero-order model**

The release of an active agent in zero-order kinetics occurs at a constant rate regardless of the active agent concentration and only depends on time.

$C_t = C_0 - k_0 t$ ***Eq 2.*** [111]

Where:

(C_t): Concentration of NF remaining at the time (t)

(C_0): Initial concentration of NF

(k_0): Zero-order release constant

(t): Time

2- First-order model

For first-order kinetics, the amount of released drug is related to the amount of remaining drug. Thus, as time passes, there is a tendency for the amount of activity released to decrease.

$Log\ C_t = log\ C_0 - \frac{k1\ t}{2.303}$ ***Eq 3.*** [111]

Where:

(C_t): Concentration of NF remaining at the time (t)

(C_0): Initial concentration of NF

(k_1): First-order release constant

(t): Time

3- Higuchi model

For Higuchi model, the rate of drug release from a matrix, usually a polymer, where the loading of solute exceeds its solubility, Cs, in the matrix, into a surrounding fluid.

$Q = k_H t^{½}$ ***Eq 4.*** (112)

Where:

(Q): Amount of NF remaining at the time (t)

(k): Release constant of Higuchi

($t^{½}$): Square root of time

4- Ritger-Peppas and Korsmeyer-Peppas model (power law)

For the power law model, the mathematical formula for calculating the exponential relationship between release and time.

This model was formulated primarily to simulate the release of a drug molecule from a polymeric matrix. The power law model can be used to examine drug release from polymeric materials when the release mechanism is unknown or when there are multiple types of drug release phenomena involved.

$log \frac{M\,t}{M} = k + n\,log\,t$ ***Eq 5.*** (111)

Where:

($\frac{M\,t}{M}$): Fraction of NF release at the time t

(k): Constant of incorporation of structural modifications and geometrical characteristics of the system

(n): Coefficient of the Fickian diffusion exponent for a system

(t): Time

The (n) value 0.45 < n < 0.89, and 1 < n means a non Fickian (anomalous), and non Fickian (Case II), respectively, and n < 0.45 mean Fickian diffusion (Case I).

5- Peppas-Sahlin model

This release kinetics model is possible to calculate the approximate two contribution mechanisms (diffusional and relaxational) in an anomalous drug release process.

$F/R = k_1 t^m + k_2 t_2^{2m}$ ***Eq 6.*** (113)

Where:

(F/R): Fraction of NF release at the time t from a diffusional and relaxational process

($k_{1,2}$): Kinetics constants

(m): Coefficient of the Fickian diffusion exponent for a system

(t): Time

The (m) value 0.45 < m < 0.89, and 1 < m means a non Fickian (anomalous), and non Fickian (Case II), respectively, and m < 0.45 mean Fickian diffusion (Case I).

The formulas that showed comparable drug release to the control (aqueous NF solution) were chosen for further studies.

2.3.3.12. Trans nasal drug permeation study

The trans nasal permeation study of NF in situ nasal gel was carried out using sheep nasal epithelium membrane. The nasal cavity of the sheep was procured from the slaughterhouse. The nasal septum was carefully removed from these nasal chambers without causing any damage to it. The nasal epithelial membrane was then carefully separated from the underlying bone, completely cleaned, and kept in a pH 7.4 cold saline buffer.

The nasal epithelial membrane was securely fastened at one end of the hollow cylindrical tube (2 cm in diameter). After that, the cylinder tube was suspended into10 mL of phosphate buffer saline (PBS) at 37 °C and adjusted to rotation at 50 rpm. NF in situ nasal gel equivalent to 20 mg NF (1 mL) was applied over the epithelium membrane.

At a time interval, every 30 min, 1 mL aliquots of receptor fluid were withdrawn over 6 h and were replaced with an equal volume of fresh PBS maintained at 37 °C. Aliquots of withdrawn samples were filtered and diluted suitably with PBS and analyzed for drug concentration spectrophotometrically double beam UV-Vis spectrophotometer at lambda max [110].

The effective permeability coefficients and flux values at steady state (linear potion of curve) were calculated from the slope according to **Eq 7 and Eq 8**, respectively.

$J_{ss} = \left(\frac{\Delta y}{\Delta x}\right)$ ***Eq 7.*** [16]

$(P_{eff}) = J_{ss} / C_0$ ***Eq 8.*** [16]

Where:

(J): Flux at steady state (mg/cm^2 min)

$\left(\frac{\Delta y}{\Delta x}\right)$: Slope of linear portion for Cumulative permeated amount (mcg/cm2/min) versus time (min)

(C_0): Initial concentration of the drug on the apical side (mg/mL)

(P_{eff}): Effective permeability coefficient (cm/min)

2.3.3.13. Fourier Transform Infrared Spectroscopy (FTIR) and Drug–Excipients Compatibility Studies

FTIR is an effective method for identifying pure compounds and compatibility studies between the active pharmaceutical ingredient (API) and the excipient(s) [136].

The FTIR spectrum of NF nasal gel of the selected formulas and the excipients used were recorded using an FTIR spectrometer between spectral bands 4000 - 400 cm^{-1}. The sample was mixed in a mortar with potassium bromide (KBr), then compressed into a tiny disc using a hydraulic press.

FTIR was carried out on several separated formulas observed by appearance test to compare its FTIR spectra with the original spectra of drug and polymers.

2.3.3.14. Stability study

The physical and chemical stability of the created in situ nasal gel was tested using stability studies. A significant amount of in situ gel was kept in screw-capped vials and stored for three months at various temperatures, 4±3°C, 25±3°C, 40±3°C. The physical stability, including appearance, color, pH, $T_{sol-gel}$ temperature, viscosity, and drug content, were studied [(110)].

2.3.4. Statistical Analysis

The results of the research were given as mean values ± standard deviation (SD) and examined according to the one-way analysis of variance (ANOVA) at which significant results ($p<0.05$) and non-significant ($p>0.05$).

Chapter Three

Results and Discussions

3 Results and Discussions

3.1. Characterization of NF

3.1.1. The melting point of NF

The melting point of NF measurement by using the capillary method was found to be 260 °C, which coincides with the reported melting point [93], which indicated the purity of drug powder.

3.1.2. Differential Scanning Calorimetry (DSC) of NF

The DSC of NF, shown in Figure 14, agrees with the reference that it exhibits an endothermic peak at 259.8°C [116]. both melting point and DSC give good evidence for the purity and crystallinity of drug powder.

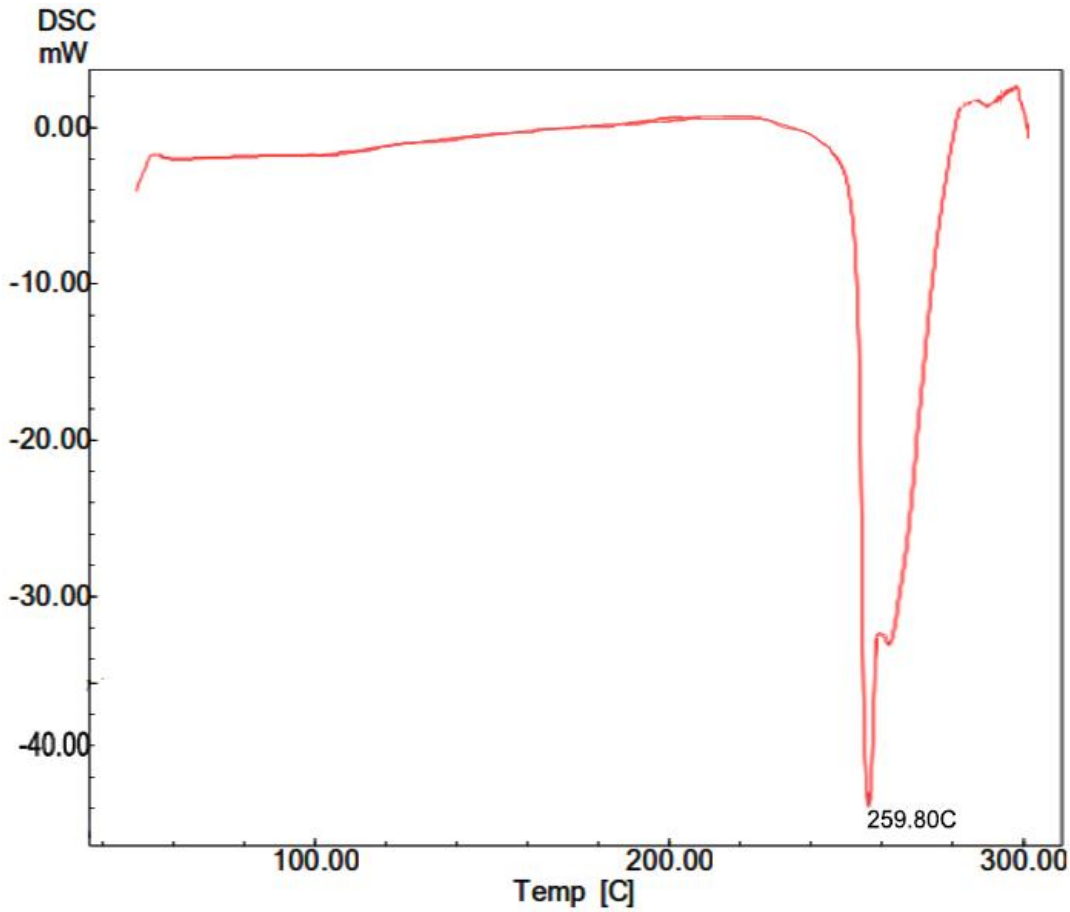

Figure 14. DSC thermogram of NF

3.1.3. The λ_{max} of NF

NF shows a maximum absorption peak at 266 nm, as shown in Figure 15,16, and 17 in deionized water, SNF, and Phosphate buffer saline, respectively.

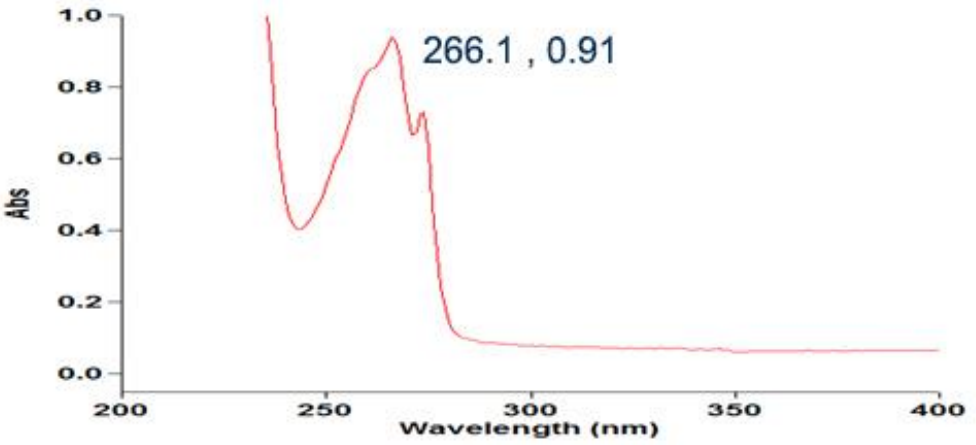

Figure 15. The UV-Vis scan of NF in deionized water

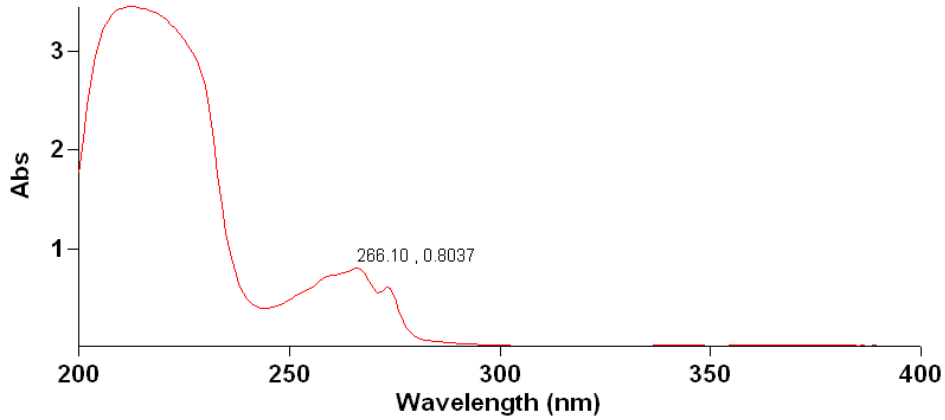

Figure 16. The UV-Vis scan of NF in buffer

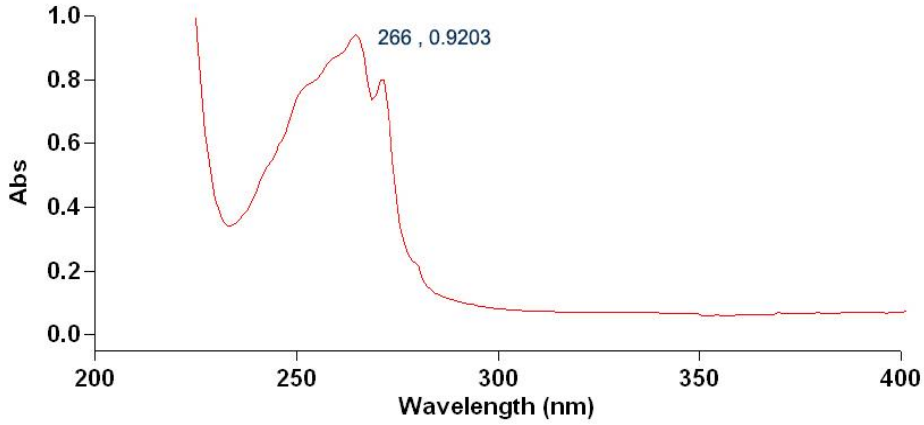

Figure 17. The UV-Vis scan of NF in SNF

Nefopam gave a single distinct peak with good absorbance in the recorded UV spectrum. The wavelength of maximum absorbance (λ max) for the drug was found to be 266 nm. That is compatible with the results of references [117,118].

3.1.4. Calibration curves of NF in different media

The Calibration curves were carried out on deionized water pH 7, phosphate buffer saline pH 7.4, and SNF pH 6.5; Figure 18 represent these curves with their trendline equations.

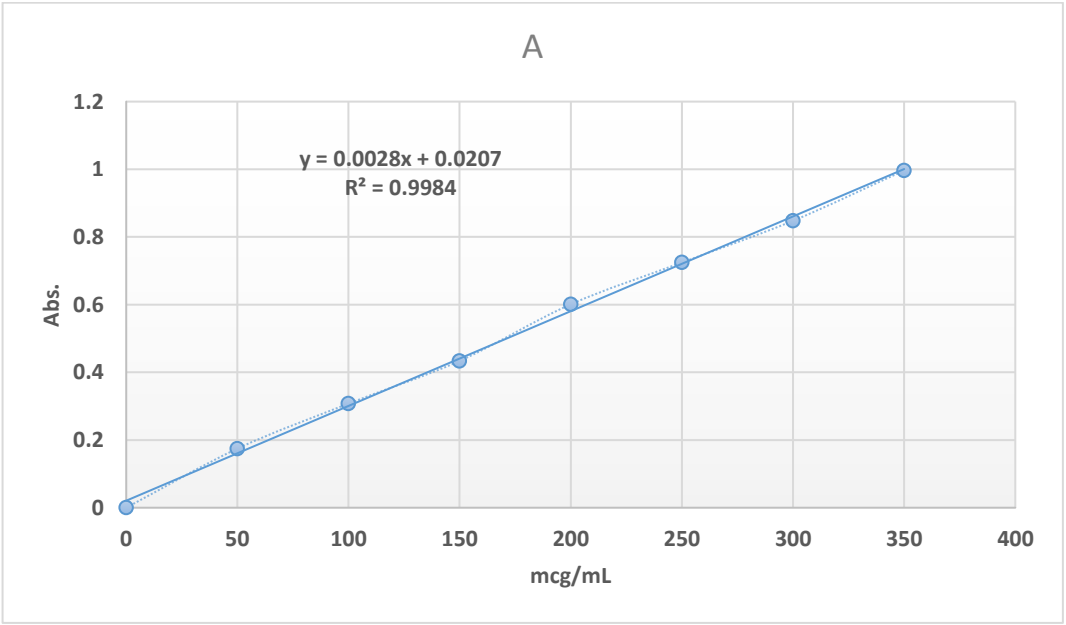

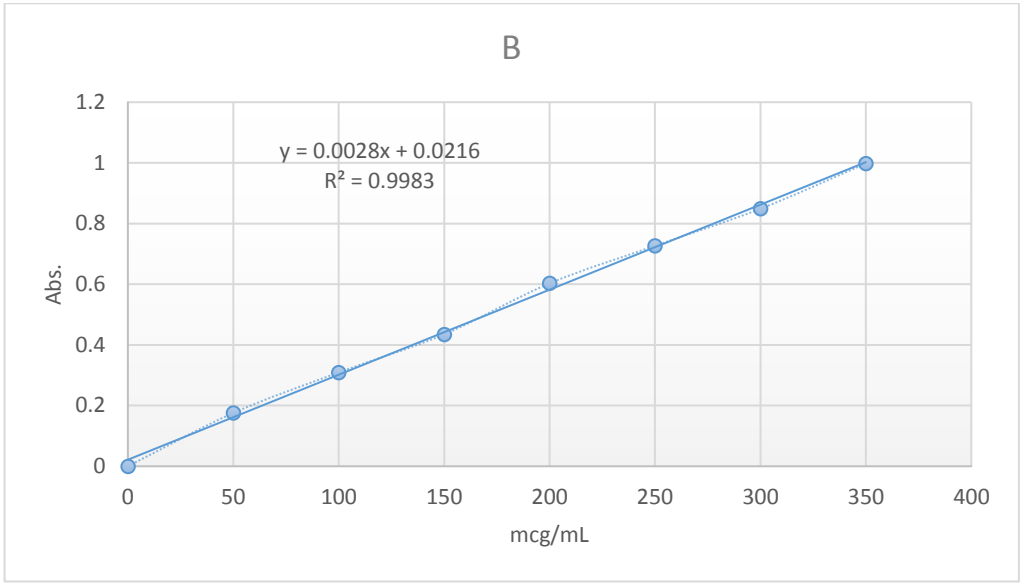

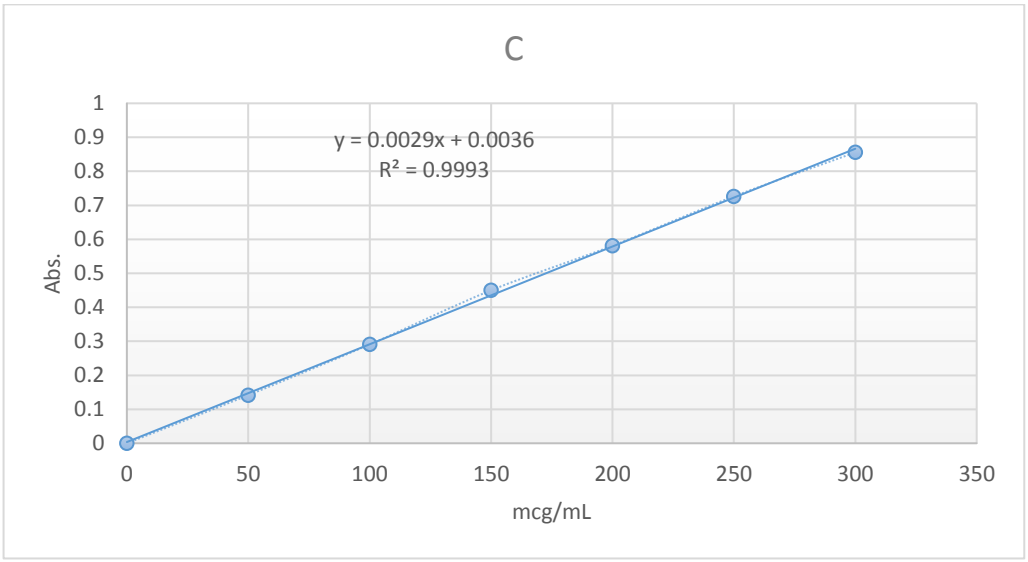

Figure 18. Standard calibration curves of NF in deionized water (A), PBS (pH 7.4) (B), and SNF (pH 6.5) (C)

Straight lines were obtained by plotting the absorbance versus concentration with high regression coefficient. This indicates that calibration curves obey Beer's law within the range of concentration used.

3.1.5. Saturated solubility measurement

The solubility of NF in aqueous buffer at pH 7.4, simulated nasal fluid pH 6.4, and deionized water pH 7, shown in Table 5.

Table 5. Saturated Solubility of NF in Different Solvents.

Solvent	Saturated solubility (mg/ml) (Mean±SD, n=3)
Aqueous buffer	21.957 ± 0.05
SNF	13.2 ± 0.11
Deionized water	21.679 ± 0.07

The fact that only (100 – 250 µl) can be instilled in a human nose [6] makes a potent drug with high solubility essential for nasal formulations [6].

3.2. Characterization of NF Nasal Formula

3.2.1. Sol-Gel Gelation temperature

Gelation temperature is the temperature at which the liquid is converted to a gel to be suitable for nasal delivery of NF The gelation temperature range suitable for nasal formulation would be 32-34ºC.

Initially, the sol-gel temperature was measured for polymer mixtures composed of only poloxamer 407 and poloxamer 188, as shown in Table 6.

Only the formulas with gelation temperature of 30-36°C [101] were selected for further addition of mucoadhesive polymers and NF.

Table 6. Gelation Temperature for Nasal In-Situ Gel Polymer Mixture

P No.	PoloX 407 (%w/v)	PoloX 188 (%w/v)	D.W q.s ml	Sol-Gel $_{Tem}$ (Mean±SD, n=3)
1	17		10	32.1 ± 0.653
2	18		10	29.5 ± 0.430
3	19		10	27.3 ± 0.120
4	20		10	23.8 ± 0.115
5	17	4	10	42.4 ± 0.346
6	18	4	10	38.5 ± 0.152
7	19	4	10	35.1 ± 0.247
8	20	4	10	28.4 ± 0.432
9	17	3	10	40.6 ± 0.461
10	18	3	10	36.0 ± 0.154
11	19	3	10	32.3 ± 0.280
12	20	3	10	27.8 ± 0.316

Table 6 revealed that PoloX 407 or PoloX 188 alone could not provide a suitable gelation temperature; only formula (P No. 1) with (17% PoloX 407) shows gelation temperature at a suitable range. In cases of mixtures of PoloX 407 and PoloX 188, several formulations (P No. 7,10 and 11) are gelled at the included temperature; these results were reported previously by Karim A. Soliman et al. where they found that PoloX 407 or PoloX 188 alone have an unsatisfactory sol-gel temperature [(119)].

Table 7. Sol-Gel (G-S) Gelation Temperature and Appearance (Mean ±SD, n=3)

F. No.	PoloX 407(%)	PoloX 188(%)	HPMC K4M (%)	HA (%)	Car934 (%)	MC (%)	S-G temp (°C)	APP*
1	17		1				33.9 ±0.113	- ppt.
2	19	4	1				40.1 ±0.425	- ppt.
3	18	3	1				38.2 ±0.236	- ppt.
4	19	3	1				34 ± 0.364	-- ppt.
5	17		0.75				33.2 ±0.168	- ppt.
6	19	4	0.75				39.4 ±0.536	- ppt.
7	18	3	0.75				40.2 ±0.325	- ppt.
8	19	3	0.75				33.1 ±0.364	- ppt.
9	17		0.5				33.2 ±0.424	- ppt.
10	19	4	0.5				40.2 ±0.244	- ppt.
11	18	3	0.5				41.3 ±0.461	- ppt.
12	19	3	0.5				32.2 ±0.145	- ppt.
13	17			0.75			34.1 ±0.295	+
14	19	4		0.75			41.2 ±0.196	+
15	18	3		0.75			42.1 ±0.325	+
16	19	3		0.75			34.2 ±0.212	++
17	17			0.5			33.2 ±0.315	++
18	19	4		0.5			40.4 ±0.213	+
19	18	3		0.5			41.5 ±0.116	++
20	19	3		0.5			34 ± 0.187	+
21	17			0.25			34 ± 0.285	++
22	19	4		0.25			41.9 ±0.314	++
23	18	3		0.25			39.8 ±0.412	++
24	19	3		0.25			33.9 ±0.440	++
25	17				0.3		34.8 ±0.173	- ppt.
26	19	4			0.3		41.7 ±0.238	-- ppt.

F. No.	PoloX 407(%)	PoloX 188(%)	HPMC K4M (%)	HA (%)	Car934 (%)	MC (%)	S-G temp (°C)	APP*
27	18	3			0.3		42 ± 0.315	-- ppt.
28	19	3			0.3		34 ± 0.164	-- ppt.
29	17				0.2		34 ± 0.253	- ppt.
30	19	4			0.2		42.1 ±0.426	-- ppt.
31	18	3			0.2		40.2 ±0.154	- ppt.
32	19	3			0.2		33.1 ±0.332	- ppt.
33	17				0.1		33.9 ±0.227	- ppt.
34	19	4			0.1		37.8 ±0.463	-- ppt.
35	18	3			0.1		38.9 ±0.352	- ppt.
36	19	3			0.1		33.1 ±0.109	- ppt.
37	17					0.3	35.9 ±0.267	+
38	19	4				0.3	39 ± 0.315	+
39	18	3				0.3	40.7 ±0.573	+
40	19	3				0.3	38.8 ±0.012	+
41	17					0.2	34 ± 0.173	+
42	19	4				0.2	38.5 ±0.532	+
43	18	3				0.2	38.9 ±0.425	+
44	19	3				0.2	34 ± 0.316	+
45	17					0.1	33.1 ±0.305	++
46	19	4				0.1	35.7 ±0.311	+
47	18	3				0.1	36.9 ±0.130	+
48	19	3				0.1	35.8 ± 0.18	+

***(Cloudy -, Very Cloudy - -, Clear +, Transparent ++, Precipitate(ppt.))**

If the gelation temperature is lower than 32°C, gelation occurs at room temperature leading to difficulty in manufacturing, handling, and administering. If the gelation temperature is greater than 34°C, the formulation will remain as a liquid at body temperature, resulting in nasal drainage. Drug and additives may increase or decrease gelation temperature; Therefore, the formulation must have a gelation temperature in the range of 30-36°C (Table 6) to allow the study of the effect of drug and additives on gelation temperature. And the formulation of Table 7 must have a gelation temperature of 32-34°C.

For the same reasons mentioned above, any formula above 36°C or below 30°C from the formula of Table 6 and any formula of Table 7 above 34°C or below 32°C were excluded from further studies.

Table 6 and 7 shows that as the concentration of PoloX 407 increase, the gelation temperature decreases due to aggregation and formation of critical gel concentration (cgc), which become more easily as the concentration increases, whereas increasing the concentration of PoloX 188, HPMC K4M, HA, MC, and Carb934, the Sol-Gel temperature increased because these polymers will build up inside a gel texture of PoloX 407 and inhibit gel formation so that the critical gel temperature will be higher [120].

3.2.2. Clarity and Appearance

Formulas were suspected for appearance and compatibility before further studies were done, Table 7 show the appearance of these formulas.

Appearance and clarity tests reveal the formation of cloudy and precipitate at the bottom of the container for formulas that contain HPMC K4M and Car 934 in all concentrations.

Table 7 shows that formula No. (F1-12) and (F25-36) were cloudy with precipitate; Figure 19 and 20 show the formation of precipitation in contrast with the transparent formula.

To know the reason behind the cloudy appearance with precipitation, one selected formula for HPMC K4M (F No. 4) and Car 934 (F No. 26) were taken for FTIR study.

Figure 19. The appearance of HPMC K4M (A) and HA (B) formulas.

Figure 20. The appearance of Carbopol 934 (A) and HA (B) formulas.

3.2.3. Gelling capacity and gelation time

Gelation time is an important feature as gelation temperature because the formula should transform into a gel upon instillation but also remain as a gel for the period of time sufficient for the drug release. Only clear and un precipitated formulas were checked. Gelation time and capacity are described in Table 8.

Table 8. Gelling Capacity, pH, Drug content, and Osmolarity of Formulas (Mean ± SD, n=3)

F No.	Gelation time (Sec.)	Gelling capacity (hr.)	pH	Drug content (w/v%)	Osmolarity mOsm/l
13	56.66 ± 2.886	6:15 ± 0.00	5.7 ± 0.24	100.44 ± 0.90	543 ± 0.081
16	60 ± 0.00	6.1 ± 0.086	5.8 ± 0.15	99.62 ± 0.460	590 ± 0.102
17	46.66 ± 2.886	5.2 ± 0.173	5.9 ±0.216	101.54 ± 1.03	484 ± 0.119
20	48.33 ± 2.886	4:15 ± 0.00	5.9 ±0.022	102.623 ±0.46	552 ± 0.258
21	46.66 ± 2.886	5.1 ± 0.086	6.1 ±0.171	102.98 ±0.582	403 ± 0.317
24	40 ± 0.00	3.63 ± 0.317	6.1 ±0.142	98.95 ± 1.138	461 ± 0.163
41	50 ± 0.00	5.1 ± 0.086	6 ± 0.415	101.607 ±0.58	358 ± 0.401
44	46.66 ± 2.886	3.816 ±0.32	6 ± 0.104	102.28 ±0.789	396 ± 0.259
45	50 ± 0.00	5.1 ± 0.173	6.1 ±0.028	99.19 ± 0.347	311 ± 0.066

The gelation study was conducted in SNF (pH 6.5). All the formulations on contact with the gelation medium had undergone sol-to-gel transition due to the presence of gel-forming polymers such as poloxamer. Gelation characteristics of the formulations showed that increasing the concentration of poloxamer increased the gelation time, while the addition of poloxamer 188 decreasing gelling capacity, as seen in Table 8. Also, the rise in the concentration of HA and MC increased the time of gelation for the formulas [(121)].

3.2.4. pH of NF nasal formulas

The degree of ionization of a drug molecule intended to be administered intranasally depends on two factors, the dissociation constant of the drug and the pH value [122] of nasal fluid (4.5-6.5) [27].

The pH value of the formula plays a significant role in the ionization process of the molecule so that it will affect its solubility and penetration capacity; the nasal formulation should have a controlled pH range (4.5-6.5) to be tolerable [27]. Increased pH increases the likelihood of nasal cavity infections by inhibiting the lysozymes responsible for eliminating them, while a decrease in their value will irritate the tissue [12].

The pH range of selected formulas 5.7-6.1, as shown in Table 8, are accepted to be used intranasally and compatible with the nasal pH range 4.5 – 6.5 [27]; at this pH range, the drug NF will be mainly in ionized form to be completely soluble in the formula.

3.2.5. Drug content of NF nasal formulas

The drug content was found to be (98.95-102.98%) which is in the acceptable range according to USP of all the formulations [123]. This indicates that the process employed in this study was capable of producing gels with uniform drug content and minimal variability, as seen in Table 8. Also, no differences were shown among upper, middle, and lower samples, which indicate a good uniform distribution of the drug.

3.2.6. Osmolarity of NF nasal formulas

The results of osmolarity were ranged from 311-590 which is within an acceptable range as shown in Table 8; osmolarity is directly proportional to the concentration of thermosensitive and mucoadhesive polymers, with HA showed the greatest impact on osmolarity [124].

3.2.7. Gel strength of NF nasal formulas

The suitable gel strength is very important for the formulation of nasal formulas. Table 9 shows the data of gel strength.

Table 9. Gel Strength and Spreadability of Formulas (Mean±SD,n=3)

F No.	Gel strength (sec.)	Gel spreadability (cm)
13	44 ± 1.414	4.25 ± 0.204
16	53.33 ± 1.247	3.86 ± 0.125
17	37.33 ± 0.943	4.63 ± 0.125
20	47.33 ± 0.471	4.36 ± 0.250
21	35.66 ± 2.05	5.16 ± 0.250
24	41 ± 0.816	4.3 ± 0.294
41	36.66 ± 0.471	5.63 ± 0.188
44	42 ± 1.414	5.26 ± 0.205
45	31 ± 0.816	5.33 ± 0.169

As the total concentration of polymers increased, the gel strength increased; this might be related to the formation of more interlocking forces (hydrogen bond, Van der Waals) between the poloxamer and mucoadhesive polymers [(125)].

Amongst the polymers studied, HA (F No. 20) showed higher gel strength as compared to MC.

3.2.8. Spreadability of NF nasal formulas

An inverse relationship between spreadability and polymer concentrations is shown in Table 9, this effect might be explained according to the viscosity enhancing effect of polymers, and the rate of spreading is inversely proportional to viscosity. All formulations have acceptable spreadability (2.5-7 cm), and these results agreed with the reported data [126].

3.2.9. Mucoadhesive strength

The residence time of the formulas in the nose can be prolonged by the mucoadhesive force of the gel. The mucoadhesive force of the formulas should be enough to supply good opposition to the gel mucociliary clearance.

The formulas mucoadhesive force is a result of hydrogen bond between polymer in formula and oligosaccharide sequence of mucin glycoprotein in the mucus membrane. Table 10 shows the mucoadhesive force of the selected formulas. Assessment of the mucoadhesive strength in terms of detachment stress revealed the increase in mucoadhesive properties of formulations with increased concentration of mucoadhesive polymer. Mucoadhesive strength for formulations containing HA (F No. 13,16,17,20,21, and 24) shows two-three fold higher mucoadhesive detachment force than that of formulations that contain MC (F No. 41,44, and 45) due to the HA ability to comprise hydrogen bonding, high molecular weight, and a semi-flexible chain [127].

Also, poloxamers have shown a mucoadhesive effect. The rapid fluid uptake from the mucus layer enabling the polymer chain to penetrate the mucin network and establish adhesive bonds has a key role in mucoadhesion; it is speculated that the higher mucoadhesive strength of the delivery system may lead to prolonged retention and increased absorption across mucosal tissues [128].

Excessive mucoadhesive force (i.e., greater than 10,000 dyne/cm^2 gel can damage the nasal mucosal membrane [128]. None of our formulations

topped the upper limit and hence appeared as formulations with optimal mucoadhesion properties.

Table 10. Mucoadhesive Force of Formulas. (Mean±SD, n=3)

F No.	Detachment weight (g)	Mucoadhesive force (dyne/cm^2)
13	7.03 ± 0.055	8776.31
16	7.52 ± 0.170	9388.03
17	6.48 ± 0.271	8089.68
20	7.31 ± 0.320	9125.86
21	6.01 ± 0.076	7502.93
24	6.73 ± 0.176	8401.78
41	2.77 ± 0.116	3458.09
44	3.55 ± 0.273	4431.85
45	2.63 ± 0.079	3283.31

3.2.10. Rheological studies

The viscosity data of selected formulas (F13-45) at liquid and gel phases under different shear rates (rpm) are shown in Table 11 and Figure 21; all formulas form solution with low viscosity at room temperature, while a significant increase in viscosity at gelation temperature. In situ gel dissent the Arrhenius equation relates the viscosity and temperature due to the presence of thermosensitive polymers that form a gel and increase viscosity when temperature increases [129].

Table 11. The Viscosity of Liquid Form for Formulas at Room Temperature, at 10 rpm, (Mean±SD, (n=3)).

F No.	Spindle No.	Viscosity (cP)
13	R5	1435.66 ± 10.530
16	R5	1579.33 ± 11.440
17	R5	1319.66 ± 13.573
20	R5	1404.66 ± 4.189
21	R5	1249.33 ± 4.988
24	R5	1314.66 ± 3.680
41	R4	1381 ± 6.164
44	R4	1366.33 ± 8.993
45	R4	1253.33 ± 3.399

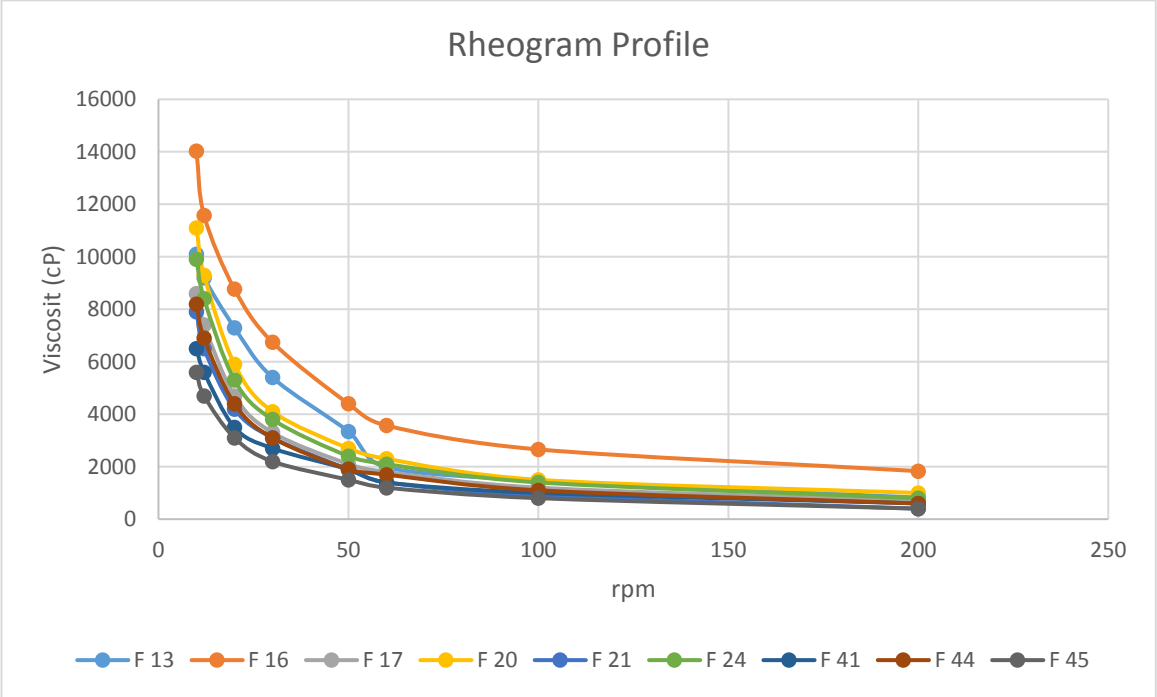

Figure 21. Rheogram profiles for formulas

The rheogram profiles of different polymers used in this study showed that as the rotation speed increased (shear rate) (Figure 21), the viscosity decreased, indicating the pseudoplastic (shear thinning liquids) flow of the preparation [130]. Formulas (F13-24) containing HA show higher viscosity in

concentration dependent manner at both room temperature and 34°C [131] than formulas (F41-45), also poloxamers show an impact on viscosity in proportion to its concentration as a result of more physical entanglement when concentration increases [72]. F 16 show higher viscosity due to a higher concentration of HA (0.75%), PoloX 407 (19%) and PoloX 188 (3%).

3.2.11. *In-vitro* drug release of NF nasal formulas

The release could be directly related to permeation and, subsequently, to the bioavailability of a drug; Figure 22 shows the release profile for formulas (13-45), F No. 45, with a low concentration of MC (0.1%) and PoloX (17%), show the most rapid and higher release percent after 15 min., meanwhile F 16, composed of HA (0.75%) and PoloX 407,188 (19,3, respectively) show lowest and slow release to reach 80% after 65 min. Other formulas with different concentrations of mucoadhesive and poloxamer(s) show release in concentration dependent patterns, as shown in Figure 22.

An increase in gel viscosity causes a slower erosion and drug release due to trapped drug inside polymer micelle that forms at higher concentrations leading to slower drug release.

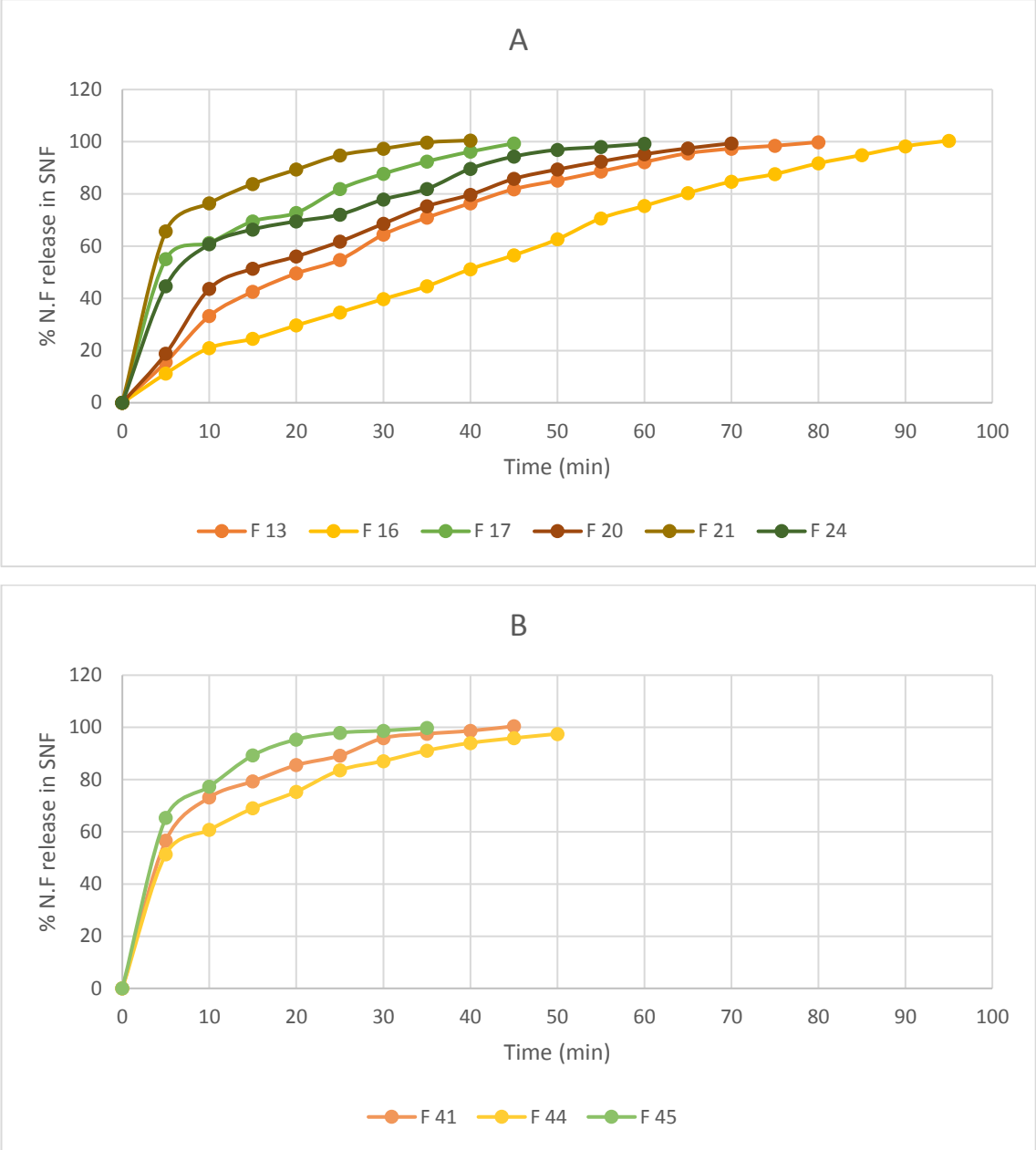

Figure 22. Graphical representation of *In-vitro* drug release study of NF from in situ nasal gel formulations, (A) HA containing formulas (F 13-24), (B) MC containing formulas (41-45) in SNF

3.2.11.1. Analysis of release mechanism

The release data were fitted to mathematical models (First-order, Zero order, Higuchi, Power law, and Peppas-Sahlin) using a DDSolver Excel Microsoft Add-in program [132] to evaluate drug release mechanism according to corresponding higher (Rsqr), lower Akaike information criterion (AIC), and coefficient exponent value (n,m) for each formula, as

shown in Table 12, dissolution profile comparison (pairwise similarity factor f2) used to compare formulas dissolution with control release profile.

Table 12. Release Mechanism Analysis by Different Models for Formulas.

Model (R^2)	F No.								
	13	**16**	**17**	**20**	**21**	**24**	**41**	**44**	**45**
Zero-order	0.7702	0.9679	0.3553	0.6979	0.0758	0.2808	0.1255	0.2544	0.1906
AIC	140.35	129.66	87.089	125.24	82.214	116.17	90.998	97.866	72.182
First-order	0.9891	0.9473	0.9240	0.9853	0.9710	0.9252	0.9738	0.9492	0.9882
AIC	88.454	139.555	65.704	79.912	51.06	86.751	55.918	68.319	38.373
Higuchi	0.9854	0.9247	0.9171	0.9875	0.8142	0.9151	0.8486	0.9016	0.8419
AIC	93.496	146.70	66.572	77.432	67.775	88.394	73.463	75.590	59.120
Power law	0.9876	0.9956	0.9942	0.9878	0.9988	0.9927	0.9960	0.9977	0.9936
n value	0.538	0.785	0.301	0.486	0.209	0.318	0.246	0.292	0.217
AIC	92.752	91.716	41.906	79.062	24.042	58.469	39.135	36.144	35.48
Peppas-Sahlin	0.9982	0.9956	0.9949	0.9928	0.9995	0.9930	0.9988	0.9980	0.9987
m value	0.807	0.397	0.225	0.677	0.325	0.242	0.415	0.367	0.460
AIC	62.103	93.708	42.598	73.2018	18.7381	59.9901	29.4134	36.7007	24.9664
Similarity factor, f2	16.20	11.18	33.33	19.33	52.84	30.06	44.17	33.15	60.66

Based on the statistically higher r^2 and lower AIC, it is possible to get the mechanism by which the drug release is governed. Table 12 shows that all formulas are best fitted to the Peppas-Sahlin model; in other words, the release mechanism is a contribution of two mechanisms (diffusional and relaxational) release process.

$F/R = k_1 t^m + k_2 t_2^{2m}$ ***Eq 9.*** (113)

Where:

(F/R): Fraction of NF release at the time t from a diffusional and relaxational process

($k_{1,2}$): Kinetics constants

(m): Coefficient of the Fickian diffusion exponent for a system

(t): Time

The (m) value $0.45 < m < 0.89$, and $1 < m$ means a non-Fickian (anomalous) and non-Fickian solvent release (Case II and super Case II), respectively, and $m < 0.45$ mean Fickian diffusion (Case I).

The formulas No. (16,17,21,24,41,44, and 45) have $m < 0.45$, so it shows Fickian release process, Fickian diffusional release occurs by the usual molecular diffusion of the drug due to a chemical potential gradient.

The formulas No. (13, and 20) have $0.45 < m < 0.89$, so it shows Case II non-Fickian **r**elaxational release process its mechanism associated with stresses and state-transition in hydrophilic polymers which swell in SNF, attributed to the erosion of the hydrophilic polymer which takes place after complete hydration of the outer layer, and then the gel layer start to disperse due to an attrition process (132).

Similarity factor f2 shows that F No. (13,16,17,20,24,41, and 44) have $f2 < 50$, which means these formulas have a different release profile from the control, meanwhile, F No. (21, and 45) has $f2 > 50$, so it has a similar release profile to the control.

As a formulation intended to be used for pain killer with a rapid release, not sustained, so only the formulas that show a similar release profile with the control was chosen for further studies.

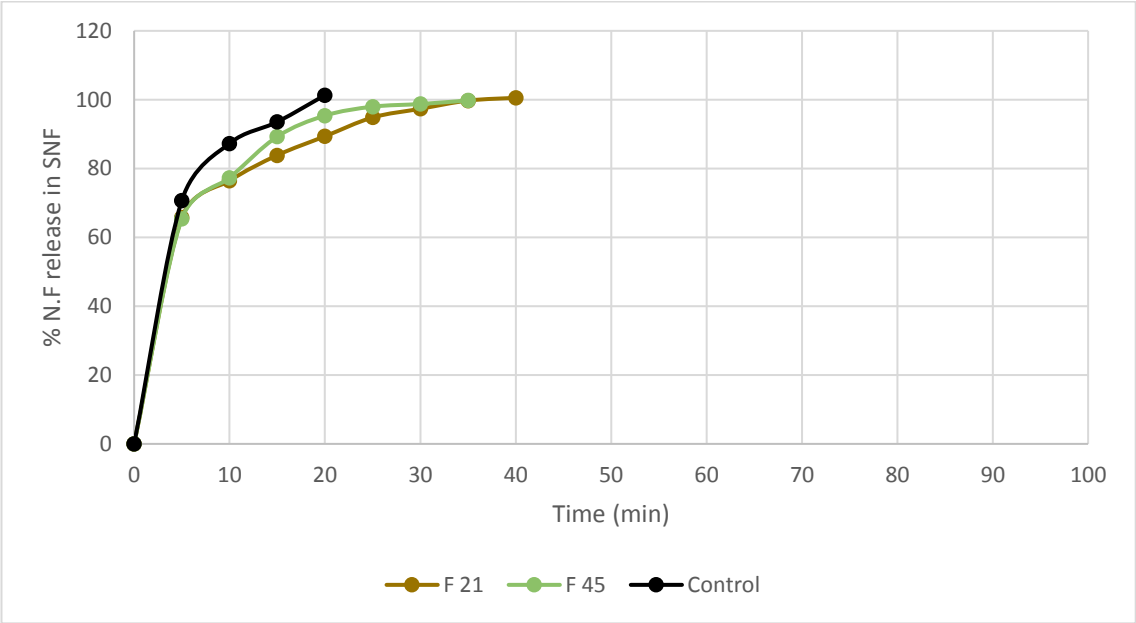

Figure 23. Graphical representation of *In-vitro* drug release study of NF from in situ nasal gel formulations (F 21,45) and free control release in SNF

The percentage of NF released from control (aqueous NF solution alone) was compared with that from formulas using the dialysis membrane.

A faster release from the control was obtained with similarity in comparison with that from the selected formulas (F21 and 45).

The percent of drug release from the control was 101.32% at 20 min in comparison with the percent of drug release from F 45, which was 99.78% at 35 min and with F 21 100.53% at 40 min, as shown in Figure 23, due to the viscosity effect as explained above.

3.2.12. Trans nasal drug permeation study

The permeation from nasal preparations were investigated. The cumulative amount over time profiles were plotted as shown in Figure 24. A linear profile (steady state) was observed during a 6-hour period, and the slope of the linear portion of the curve was determined by linear regression.

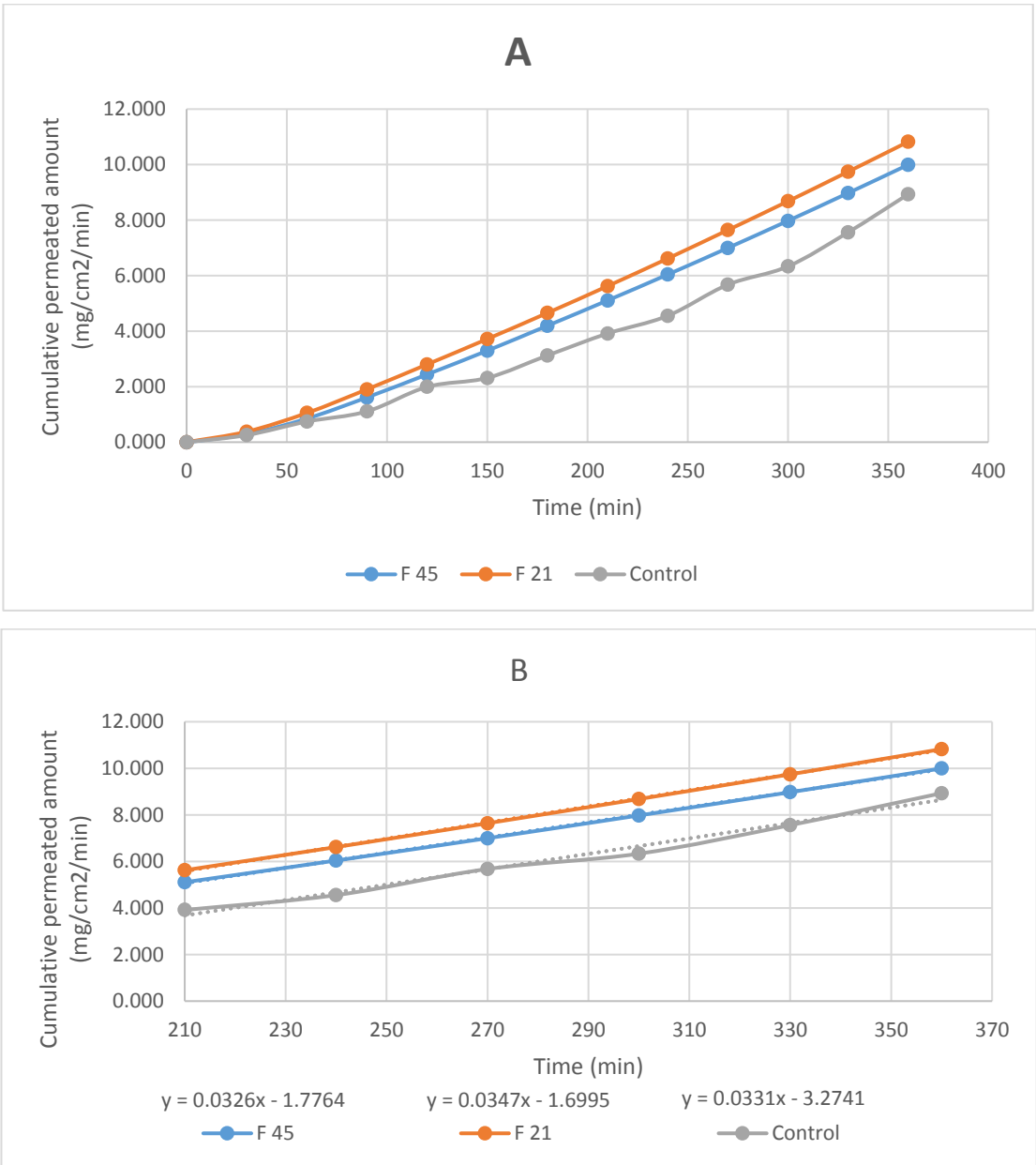

Figure 24. Cumulative permeation of NF from F 21 and 45 through nasal mucosa (A), Linear portion of permeation curve (steady state) (B).

The slope of the observed straight line of the curve was determined by linear regression Table 13. The effective permeability coefficients and flux values at a steady state were calculated from the slope according to the equations **Eq 7** and **Eq 8**, respectively.

Table 13. *Ex-vivo* Permeation Parameters for Selected Formulas.

F No.	J_{ss} (mg/cm^{2}min)	P_{eff} (cm/min)
Control	0.0331	$1.655 * 10^{-3}$
F 21	0.0347	$1.735 * 10^{-3}$
F 45	0.0326	$1.63 * 10^{-3}$

Permeation results revealed that F No. 21 and 45, as well as the control, show the initial high flux value followed by a decrease in value after about 90 min, as shown in Figure 24 and Table 13.

The contact of the fresh surface of the drug present in formula to the sheep mucosa cause initial rapid permeation and sustained drug permeation after 90 min due to the thermosensitive polymer like PoloX 407 [133] and mucoadhesive polymers included in the formula; the poloxamer slightly decreases the rate of drug release due to enhanced micellar core and gel network with a mucoadhesive polymer which entraps the drug and sustains the release [134].

3.2.13. Fourier Transform Infra-Red Spectroscopy (FTIR) and Drug-Excipient's compatibility

FTIR was carried out on drug and polymers powder, as shown in Figure 25 and 26.

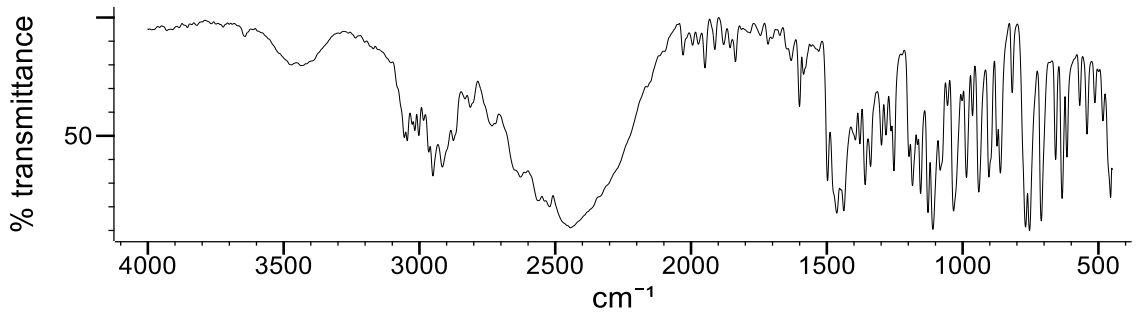

Figure 25. FTIR of NF

Spectra is compatible with the characteristics absorption peaks of NF FTIR spectra, at 3440 cm^{-1} ,3049 cm^{-1} , 2947 cm^{-1} , 2440 cm^{-1} , 1464 cm^{-1} , 1437 cm^{-1} , 1357 cm^{-1}, 1107 cm^{-1} , 1028 cm^{-1} , and 760 cm^{-1} ,correlates to C-O-C of ring,substituted aromatic ring, C-H of alkane(s), resonance of amine salt NH^{+} , C=C of substituted aromatic ring, C_3-N, C-O stretch of cyclic ether,o-disubstituted aromatic ring, and mono-substituted and o-disubstituted aromatic rings, respectively. These findings were superimposed with the reported peaks [116].

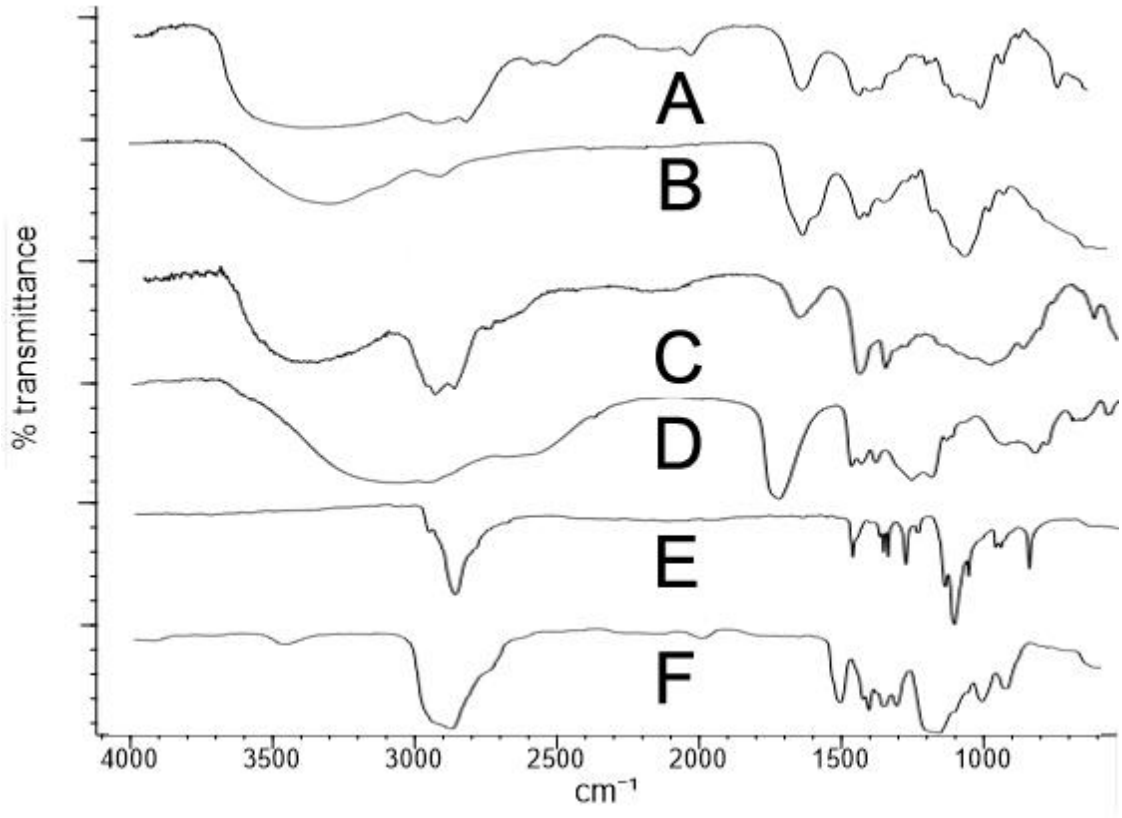

Figure 26. FTIR for HPMC K4M (A), HA (B), MC (C), Car934 (D), PoloX 407 (E), and PoloX 188 (F)

Spectra show characteristics peaks of HPMC at 3650-2800 cm^{-1} broad peak, 1653 cm^{-1}, 1450 cm^{-1}, and 1026 cm^{-1}, that are corresponded to a broad range of hydroxyl H-bond that overlap and cover sp^3 C-H stretching of alkane, cellulose nitrate ester group that converted from cellulose hydroxyl groups, spectra of poly- (vinyl alcohol) O-H deformation spectra of a secondary alcohol, and C-O-C spectra, respectively. Spectra coincide with reported peaks [135].

HA peaks at 3500-3000 cm^{-1},2891 cm^{-1}, 1603 cm^{-1}, and 1030 cm^{-1} are indicated for broad spectra of H-bond of hydroxyl of acidic, alcoholic, and amine groups of hyaluronate, C-H stretching of ring moieties, COOH group of an acidic group, and C-O-C ether group. That agrees with reference [136].

MC peaks at 3600-3050 cm^{-1},2926 cm^{-1}, 1640 cm^{-1}, 1456 cm^{-1}, and 1046 $cm^{-1;}$ these are spectra for broad H-bond spectra of acidic and alcoholic -O.H. groups that overlap weak C-H stretching peak at 3000-3100 cm^{-1}, C-

H stretching of cyclic alkane, cellulose nitrate ester group that converted from cellulose hydroxyl groups, poly- (vinyl alcohol), and C-O-C peak, respectively. These peaks are compatible with the reported peaks [137].

Car934 peaks at 3500-2500 cm^{-1}, 1711 cm^{-1}, and 1165 cm^{-1}, correlate to carboxylic dimer H-bond COOH that hide sp^3 C-H stretching peak, C=O, and C-O stretching mode, respectively. That is match the reported Car934 peaks [135].

PoloX 407 and PoloX 188 have two characteristic peaks that appear at 2868 cm^{-1} and 1100 cm^{-1}, representing the reading of R-CH_3 and C-O-C peaks.

Physicochemical compatibility between NF and different excipients was studied using FTIR to examine any interactions between the NF and the excipients used in the formulation. The spectrums were compared to the spectrum of NF alone.

FTIR spectra of F **No. 21 and 45** are shown in Figure 27, and spectra of **F No. 4 and 26** are shown in Figure 28.

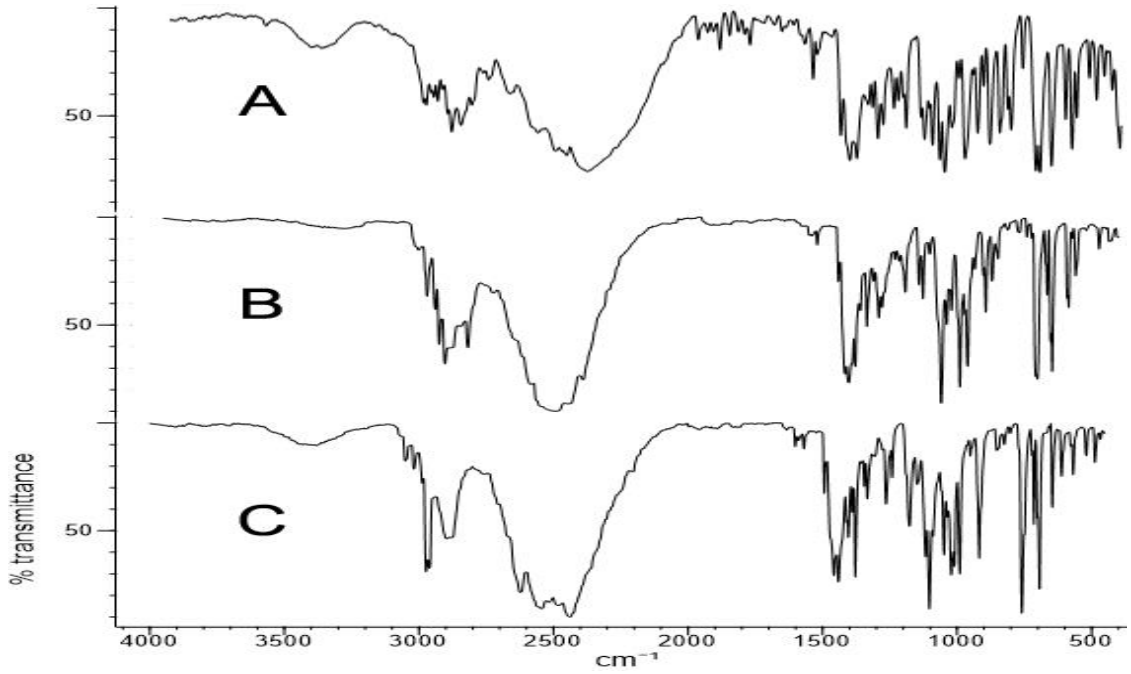

Figure 27. FTIR of NF (A) F No. 21 (B) and F No. 45 (C)

Characteristics peaks of NF, as explained above, appear at its locations on spectrums, which means there are no significant interactions between NF and polymers used in F No. 21 and 45.

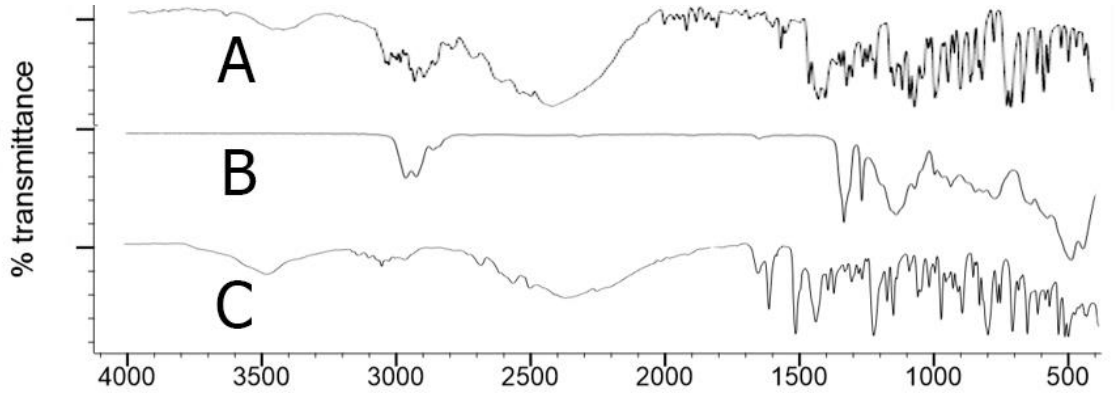

Figure 28. FTIR of NF (A), F No. 4 (B) and F No. 26 (C).

In comparing with FTIR of pure drug Figure 25, we found that a peak has lower intensity with the absence of peaks at 2800 cm^{-1} – 1460 cm^{-1} region and absence of a characteristic peak at 1000 cm^{-1} – 1100 cm^{-1} of cyclic C-O-C; these might have resulted from the interaction of NF with HPMC K4M and Car934.

Despite the critical need to verify API-excipient compatibility, there is currently no globally acknowledged standard for evaluating such interactions; FTIR and appearance are straightforward methods often used in analytical labs [(114)].

Incompatibility is characterized as a change that occurs, and an unfavorable product is produced, which may influence the pharmaceutical product's safety, effectiveness, stability, and appearance [(104)].

The FTIR spectrum of the selected formula of (F 21 and F 45) containing NF There were no significant differences in the chief characteristic bands of the drug, indicating no interaction between the drug and other additives.

3.2.14. Stability of NF nasal formulas

A stability study was carried out in a humidity-controlled chamber where the temperature was set at 40 ± 2 °C, at room temperature (25 °C ± 2 °C), and at 4 °C ± 2 °C for 3 months as shown in Table 14.

Table 14. Effect of Different Temperature on Stability of NF Nasal Formulas

F	Study		Appear.	pH	$T_{sol-gel}$	Drug content%
21	0 mon	25°C	Transparent	6.1	34	102.63
	1 mon	4°C	Transparent	6	34	100.25
		25°C	Transparent	6.1	33.5	99.93
		40°C	Transparent	6	34.2	100.42
	2 mon	4°C	Transparent	6.1	33.8	100.56
		25°C	Clear	6	34.1	98.78
		40°C	Clear	5.8	34.3	99.73
	3 mon	4°C	Transparent	6.2	33.7	97.24
		25°C	Transparent	5.9	33.3	98.71
		40°C	Clear	6	34	97.82
45	0 mon	25°C	Transparent	6	33	99.25
	1 mon	4°C	Transparent	6.1	33.3	98.36
		25°C	Clear	6.3	33.2	98.85
		40°C	Transparent	6	33.4	99.05
	2 mon	4°C	Transparent	6	32.6	97.24
		25°C	Transparent	5.9	32.4	97.78
		40°C	Transparent	6.2	33.7	96.24
	3 mon	4°C	Transparent	5.7	32.9	98.25
		25°C	Transparent	6.1	33	98.73
		40°C	Transparent	6.1	32.6	97.26

The formulations showed good stability at different temperatures. There were no changes in visual appearance, and pH remained constant within physiological nasal pH for the entire stability period; gelation temperature remained within the desired range of 32-34 ^{o}C, and drug content did not deviate by more than 2%, indicating that the drug is stable in the F formulations.

Chapter Four Conclusions

4 Conclusions and Recommendations

4.1. Conclusions

Some of the important conclusions that have been drawn from 'Results and Discussions are as follows:

1- A promising non-invasive thermosensitive nasal mucoadhesive in situ gel of nefopam hydrochloride can be prepared successfully by using poloxamer 407 based in situ gel together with mucoadhesive polymers.
2- The cold preparation method used to formulate nasal in situ gel was simple and reproducible.
3- The gelation temperature depends on the concentration of PoloX 407, 188 and mucoadhesive polymers.
4- Using HPMC K4M and Carb934 were incompatible and resulted in formation of precipitation.
5- The pH of the formulations varied from 5.7 – 6.1, which is considered safe for nasal delivery.
6- Gel strength and viscosity depend on concentrations of polymers, with HA had more mucoadhesive forces than MC.
7- Drug release kinetics analysis reveals that selected formulas follow the Peppas-Sahlin model (the release mechanism is a contribution of two mechanisms (diffusional and relaxational) release process.
8- Compatibility study for No. F 21 and 45 show no interactions between the drug and the polymers used.
9- The formulas No. F 21 and 45 showed good stability for 3 months at different storage conditions.

4.2. Recommendations for future study

1- Further studies on the compatibility of NF with HPMC K4M and Car934 are recommended.

2- *In-vivo* studies on the nasal in-situ gel of nefopam are recommended for future studies.

References

Reference

1. Agrawal M, Saraf S, Saraf S, Dubey SK, Puri A, Patel RJ, et al. Recent strategies and advances in the fabrication of nano lipid carriers and their application towards brain targeting. J. Control. Release2020;321:372–415 .
2. Uppuluri CT, Ravi PR, Dalvi A V. Design, optimization and pharmacokinetic evaluation of Piribedil loaded solid lipid nanoparticles dispersed in nasal in situ gelling system for effective management of Parkinson's disease. Int J Pharm. 2021;606(January):120881:Online .
3. Dhuria S V., Hanson LR, Frey WH. Intranasal delivery to the central nervous system: Mechanisms and experimental considerations. J Pharm Sci. 2010;99(4):1654–73 .
4. Giunchedi P, Gavini E, Bonferoni MC. Nose-to-brain delivery. Pharmaceutics2020;12(2):1–5 .
5. Crowe TP, Greenlee MHW, Kanthasamy AG, Hsu WH. Mechanism of intranasal drug delivery directly to the brain. Life Sci.2018;195:44–52 .
6. Wang Z, Xiong G, Tsang WC, Schätzlein AG, Uchegbu IF. Nose-to-brain delivery. J. Pharmacol. Exp. Ther.2019;370(3):593–601 .
7. Chatterjee B, Gorain B, Mohananaidu K, Sengupta P, Mandal UK, Choudhury H. Targeted drug delivery to the brain via intranasal nanoemulsion: Available proof of concept and existing challenges. Int. J. Pharm.2019;565:258–68 .
8. Mittal D, Ali A, Md S, Baboota S, Sahni JK, Ali J. Insights into direct nose to brain delivery: Current status and future perspective. Drug Deliv.2014;21(2):75–86 .
9. Kozlovskaya L, Abou-Kaoud M, Stepensky D. Quantitative analysis of drug delivery to the brain via nasal route. J. Control. Release2014;189:133–40 .
10. Keller LA, Merkel O, Popp A. Intranasal drug delivery: opportunities

and toxicologic challenges during drug development. Drug Deliv Transl Res. 2022;12(4):735–57 .

11. Agrawal M, Saraf S, Saraf S, Antimisiaris SG, Chougule MB, Shoyele SA, et al. Nose-to-brain drug delivery: An update on clinical challenges and progress towards approval of anti-Alzheimer drugs. J. Control. Release2018;281:139–77 .
12. Deruyver L, Rigaut C, Lambert P, Haut B, Goole J. The importance of pre-formulation studies and of 3D-printed nasal casts in the success of a pharmaceutical product intended for nose-to-brain delivery. Adv. Drug Deliv. Rev.2021;175:113826:Online .
13. Samaridou E, Alonso MJ. Nose-to-brain peptide delivery – The potential of nanotechnology. Bioorganic Med Chem. 2018;26(10):2888–905 .
14. Pardeshi CV, Belgamwar VS. Direct nose to brain drug delivery via integrated nerve pathways bypassing the blood-brain barrier: An excellent platform for brain targeting. Expert Opin. Drug Deliv.2013;10(7):957–72 .
15. Al Bakri W, Donovan MD, Cueto M, Wu Y, Orekie C, Yang Z. Overview of intranasally delivered peptides: key considerations for pharmaceutical development. Expert Opin. Drug Deliv.2018;15(10):991–1005 .
16. Inoue D, Furubayashi T, Tanaka A, Sakane T, Sugano K. Quantitative estimation of drug permeation through nasal mucosa using in vitro membrane permeability across Calu-3 cell layers for predicting in vivo bioavailability after intranasal administration to rats. Eur J Pharm Biopharm. 2020;149:145–53 .
17. Katona G, Sabir F, Sipos B, Naveed M, Schelz Z, Zupkó I, et al. Development of lomustine and n-propyl gallate co-encapsulated liposomes for targeting glioblastoma multiforme via intranasal administration. Pharmaceutics. 2022;14(3):14030631:Online .

18. Mignani S, Shi X, Karpus A, Majoral JP. Non-invasive intranasal administration route directly to the brain using dendrimer nanoplatforms: An opportunity to develop new CNS drugs. Eur. J. Med. Chem.2021;209:112905:Online .
19. Pires PC, Melo D, Santos AO. Intranasal delivery of antiseizure drugs. In: Drug Delivery Devices and Therapeutic Systems. Elsevier; 2021. page 623–46.
20. Omar MM, Eleraky NE, El Sisi AM, Hasan OA. Development and evaluation of in-situ nasal gel formulations of nanosized transferosomal sumatriptan: Design, optimization, in vitro and in vivo evaluation. Drug Des Devel Ther. 2019;13:4413–30 .
21. Long Y, Yang Q, Xiang Y, Zhang Y, Wan J, Liu S, et al. Nose to brain drug delivery - A promising strategy for active components from herbal medicine for treating cerebral ischemia reperfusion. Pharmacol. Res.2020;159:104795:Online .
22. Bhise SB, Yadav AV, Avachat AM, Malayandi R. Bioavailability of intranasal drug delivery system. Asian Journal of Pharmaceutics. 2008:201-215.
23. Gänger S, Schindowski K. Tailoring formulations for intranasal nose-to-brain delivery: A review on architecture, physico-chemical characteristics and mucociliary clearance of the nasal olfactory mucosa. Pharmaceutics2018;10(3):10030116:Online .
24. Kundi V, Ho J. Predicting octanol-water partition coefficients: are quantum mechanical implicit solvent models better than empirical fragment-based methods?. J Phys Chem B. 2019;123(31):6810–22 .
25. Moinuddin S, Hasan Razvi S, Fazil M, Mustaneer Akmal M, Syed Moinuddin C, Shanawaz Uddin M, et al. Nasal drug delivery system: A innovative approach. Pharma Innov J. 2019;8(3):169–77 .
26. Wang D, Du Y, Zhang W, Han X, Zhang H, Wang Z, et al. Development and in vivo evaluation of intranasal formulations of

parathyroid hormone. Drug Deliv. 2021;28(1):487–98 .

27. Boddu SH, Kumari S. Design and in vitro evaluation of intranasal diazepam for treating acute repetitive seizures: a technical note. J Pharm Innov. 2022;17:612-621 .
28. Pandey V, Gadeval A, Asati S, Jain P, Jain N, Roy RK, et al. Formulation strategies for nose-to-brain delivery of therapeutic molecules. In: Drug Delivery Systems. Elsevier; 2019:291–332 .
29. Zhang L, Yang S, Wong LR, Xie H, Ho PCL. In vitro and in vivo comparison of curcumin-encapsulated chitosan-coated poly (lactic-co-glycolic acid) nanoparticles and curcumin/hydroxypropyl-β-cyclodextrin inclusion complexes administered intranasally as therapeutic strategies for Alzheimer's Disease. Mol Pharm. 2020;17(11):4256–69 .
30. Martín-Sabroso C, Aparicio-Blanco J, Pires PC, Rodrigues M, Alves G, Santos AO. Academic Editors: Ana strategies to improve drug strength in nasal preparations for brain delivery of low aqueous solubility drugs. 2022;14(3):14030588:Online .
31. Kushwaha SKS, Keshari RK, Rai AK. Advances in nasal trans-mucosal drug delivery. J Appl Pharm Sci. 2011(07):21–8 .
32. Kapoor M, Cloyd JC, Siegel RA. A review of intranasal formulations for the treatment of seizure emergencies. J. Control. Release2016;237:147–59 .
33. Salade L, Wauthoz N, Goole J, Amighi K. How to characterize a nasal product. The state of the art of in vitro and ex vivo specific methods. Int. J. Pharm.2019;561:47–65 .
34. Bahadur S, Pathak K. Physicochemical and physiological considerations for efficient nose-to-brain targeting. Expert Opin. Drug Deliv.2012;9(1):19–31.
35. Saito S, Ainai A, Suzuki T, Harada N, Ami Y, Yuki Y, et al. The effect of mucoadhesive excipient on the nasal retention time of and the

antibody responses induced by an intranasal influenza vaccine. Vaccine. 2016;34(9):1201–7 .

36. Vaz G, Clementino A, Mitsou E, Ferrari E, Buttini F, Sissa C, et al. In vitro evaluation of curcumin- and quercetin-loaded nanoemulsions for intranasal administration: Effect of surface charge and viscosity. Pharmaceutics. 2022;14(1):14010149: Online.
37. Nair AB, Chaudhary S, Shah H, Jacob S, Mewada V, Shinu P, et al. Intranasal delivery of darunavir-loaded mucoadhesive in situ gel: experimental design, in vitro evaluation, and pharmacokinetic studies. Gels.2022;8(6):8060342:Online .
38. Sipos B, Csóka I, Szivacski N, Budai-Szűcs M, Schelcz Z, Zupkó I, et al. Mucoadhesive meloxicam-loaded nanoemulsions: development, characterization and nasal applicability studies. Eur J Pharm Sci. 2022;175:106229:Online .
39. Patil M. Chapter 7 - Mucoadhesion as a strategy to enhance the direct nose-to-brain drug delivery. Direct nose-to-brain drug delivery. Academic Press; 2021;115–56.
40. Kim A, Pavlova E, Kolacheva A, Bogdanov V, Dilmukhametova L, Blokhin V, et al. Development of early diagnosis of Parkinson's disease on animal models based on the intranasal administration of α-methyl-p-tyrosine methyl ester in a gel system. Biomed Pharmacother. 2022;150:11249:Online .
41. Bekhet MA, Ali AA, Kharshoum RM, El-Ela FIA, Salem HF. Intranasal niosomal in situ gel as a novel strategy for improving citicoline efficacy and brain delivery in treatment of epilepsy: In vitro and ex vivo characterization and in vivo pharmacodynamics investigation. J Pharm Sci. 2022;111(8):2258-69 .
42. Gao M, Shen · Xin, Mao S. Factors influencing drug deposition in the nasal cavity upon delivery via nasal sprays. 2020;50:251–9 .
43. Sigurdsson HH, Kirch J, Lehr CM. Mucus as a barrier to lipophilic

drugs. Int J Pharm. 2013;453(1):56–64 .

44. Hersh DS, Wadajkar AS, Roberts NB, Perez JG, Connolly NP, Frenkel V, et al. Evolving drug delivery strategies to overcome the blood brain barrier. Current Pharmaceutical Design. 2016;22:1177-93.
45. Gizurarson S. The effect of cilia and the mucociliary clearance on successful drug delivery. Biol. Pharm. Bull. 2015;38:497-506.
46. Robert-Hazotte A, Faure P, Neiers F, Potin C, Artur Y, Coureaud G, et al. Nasal mucus glutathione transferase activity and impact on olfactory perception and neonatal behavior. Sci Rep. 2019;9(1):3104:Online .
47. Heydel JM, Faure P, Neiers F. Nasal odorant metabolism: enzymes, activity and function in olfaction. Drug Metab. Rev.2019;51(2):224–45 .
48. Sekerdag E. Challenges of the Nose-to-Brain Route. In: nanotechnology methods for neurological diseases and brain tumors: drug delivery across the blood-brain barrier. Elsevier; 2017:103–13.
49. Tirucherai GS, Yang C, Mitra AK. Prodrugs in nasal drug delivery. Expert Opin Biol Ther. 2001;1(1):49–66 .
50. Erdő F, Bors LA, Farkas D, Bajza Á, Gizurarson S. Evaluation of intranasal delivery route of drug administration for brain targeting. 2018;143:155-70.
51. Pires PC, Rodrigues M, Alves G, Santos AO. Strategies to improve drug strength in nasal preparations for brain delivery of low aqueoussolubility drugs.Pharmaceutics2022;14(3):14030588:Online
52. Clementino AR, Pellegrini G, Banella S, Colombo G, Cantù L, Sonvico F, et al. Structure and fate of nanoparticles designed for the nasal delivery of poorly soluble drugs. Mol Pharm. 2021;18(8):3132–46 .
53. Bourganis V, Kammona O, Alexopoulos A, Kiparissides C. Recent advances in carrier mediated nose-to-brain delivery of pharmaceutics. Eur. J. Pharm. Biopharm.2018;128:337–62 .
54. Seju U, Kumar A, Sawant KK. Development and evaluation of

olanzapine-loaded PLGA nanoparticles for nose-to-brain delivery: In vitro and in vivo studies. Acta Biomater. 2011;7(12):4169–76 .

55. Wang S, Sun Y, Zhang J, Cui X, Xu Z, Ding D, et al. Astragalus polysaccharides/chitosan microspheres for nasal delivery: preparation, optimization, characterization, and pharmacodynamics. Front Pharmacol. 2020;11:00230:Online .
56. Costa C, Moreira JN, Amaral MH, Sousa Lobo JM, Silva AC. Nose-to-brain delivery of lipid-based nanosystems for epileptic seizures and anxiety crisis. J. Control. Release2019;295:187–200.
57. Galgatte UC, Kumbhar AB, Chaudhari PD. Development of in situ gel for nasal delivery: Design, optimization, in vitro and in vivo evaluation. Drug Deliv. 2014;21(1):62–73 .
58. Suri R, Beg S, Kohli K. Target strategies for drug delivery bypassing ocular barriers. J Drug Deliv Sci Technol. 2020;55:101389:Online .
59. Chowhan A, Giri TK. Polysaccharide as renewable responsive biopolymer for in situ gel in the delivery of drug through ocular route. Int. J. Biol. Macromol.2020;150:559–72 .
60. Al-Kinani AA, Zidan G, Elsaid N, Seyfoddin A, Alani AWG, Alany RG. Ophthalmic gels: past, present and future. Adv. Drug Deliv. Rev.2018;126:113–26 .
61. Sosnik A, Seremeta KP. Polymeric hydrogels as technology platform for drug delivery applications. Gels2017;3(3):3030025:Online .
62. Dalvi A V., Ravi PR, Uppuluri CT, Mahajan RR, Katke S V., Deshpande VS. Thermosensitive nasal in situ gelling systems of rufinamide formulated using modified tamarind seed xyloglucan for direct nose-to-brain delivery: design, physical characterization, and in vivo evaluation. J Pharm Investig. 2021;51(2):199–211 .
63. Teotia AK, Sami H, Kumar A. Thermo-responsive polymers: Structure and design of smart materials. in: switchable and responsive surfaces and materials for biomedical applications. Elsevier Inc.; 2015:3–43.

64. Soniya R., Asish Dev, S. Rathod, Ganesh D. An overview of in situ gelling systems. P and B Evaluations. 2016;3(1):60–9 .
65. Saini R, Saini S, Singh G, Banerjee A. In situ gels- a new trends in ophthalmic drug delivery systems. Int J Pharma Sci Res. 2015;6(5):886-90 .
66. Konatham M, Gorle MT, Pathakala N, Bakshi V, Mamidisetti YD, Chinthakindi P, et al. In situ gel polymers: A review. Int J Appl Pharm. 2021;13(1):86–90 .
67. Ci L, Huang Z, Liu Y, Liu Z, Wei G, Lu W. Amino-functionalized poloxamer 407 with both mucoadhesive and thermosensitive properties: preparation, characterization and application in a vaginal drug delivery system. Acta Pharm Sin B. 2017;7(5):593–602 .
68. Carvalho GC, Araujo VHS, Fonseca-Santos B, de Araújo JTC, de Souza MPC, Duarte JL, et al. Highlights in poloxamer-based drug delivery systems as strategy at local application for vaginal infections. Int. J. Pharm.2021;602:120635:Online .
69. Abuwatfa WH, Awad NS, Pitt WG, Husseini GA. Thermosensitive polymers and thermo-responsive liposomal drug delivery systems. Polymers (Basel).2022;14(5):14050925:Online .
70. Almeida M, Magalhães M, Veiga F, Figueiras A. Poloxamers, poloxamines and polymeric micelles: definition, structure and therapeutic applications in cancer. J. Polym. Res.2018;25(1):31:Online
71. Russo E, Villa C. Poloxamer hydrogels for biomedical applications. Pharmaceutics2019;11(12):11120671:Online .
72. Fakhari A, Corcoran M, Schwarz A, Fakhari A. Thermogelling properties of purified poloxamer 407. Heliyon. 2017;3:390:Online .
73. Akash MSH, Rehman K, Sun H, Chen S. Assessment of release kinetics, stability and polymer interaction of poloxamer 407-based thermosensitive gel of interleukin-1 receptor antagonist. Pharm Dev Technol. 2014;19(3):278–84 .

74. Giuliano E, Paolino D, Fresta M, Cosco D. Mucosal applications of poloxamer 407-based hydrogels: an overview. Pharmaceutics2018;10(3):10030159:Online .
75. Moghimi SM, Hunter AC, Dadswell CM, Savay S, Alving CR, Szebeni J. Causative factors behind poloxamer 188 (Pluronic F68, FlocorTM)-induced complement activation in human sera. a protective role against poloxamer-mediated complement activation by elevated serum lipoprotein levels. Biochim Biophys Acta - Mol Basis Dis. 2004;1689(2):103–13 .
76. Chen J, Zhou R, Li L, Li B, Zhang X, Su J. Mechanical, rheological and release behaviors of a poloxamer 407/poloxamer 188/carbopol 940 thermosensitive composite hydrogel. Molecules. 2013;18(10):12415–25 .
77. Brady J, Drig T, Lee PI, Li JX. Polymer properties and characterization. in: developing solid oral dosage forms: pharmaceutical theory and practice: Second Edition. Elsevier Inc.; 2017:181–223.
78. Deshmukh K, Basheer Ahamed M, Deshmukh RR, Khadheer Pasha SK, Bhagat PR, Chidambaram K. Biopolymer composites with high dielectric performance: interface engineering. in: biopolymer composites in electronics. Elsevier Inc.; 2017:27–128.
79. British Pharmacopoeia Commission. British Pharmacopoeia 2016. London: TSO; 2016.
80. Lierova A, Kasparova J, Filipova A, Cizkova J, Pekarova L, Korecka L, et al. Hyaluronic acid: known for almost a century, but still in vogue. Pharmaceutics2022;14(4):14040838:Online .
81. Rao NV, Rho JG, Um W, Ek PK, Nguyen VQ, Oh BH, et al. Hyaluronic acid nanoparticles as nanomedicine for treatment of inflammatory diseases. Pharmaceutics2020;12(10):1–18 .
82. Aguilera-Garrido A, Molina-Bolívar JA, Gálvez-Ruiz MJ, Galisteo-González F. Mucoadhesive properties of liquid lipid nanocapsules

enhanced by hyaluronic acid. J Mol Liq. 2019;296:111965:Online .

83. Bakhrushina E, Anurova M, Demina N, Kashperko A, Rastopchina O, Bardakov A, et al. Comparative study of the mucoadhesive properties of polymers for pharmaceutical use. Open Access Maced J Med Sci. 2020;8(A):639–45 .
84. Benet LZ, Broccatelli F, Oprea TI. BDDCS applied to over 900 drugs. AAPS J. 2011;13(4):519–47 .
85. Hirun N, Tantishaiyakul V, Sangfai T, Ouiyangkul P, Li L. In situ mucoadhesive hydrogel based on methylcellulose/xyloglucan for periodontitis. J Sol-Gel Sci Technol. 2019;89(2):531–42 .
86. Evans MS, Lysakowski C, Tramèr MR. Nefopam for the prevention of postoperative pain. Br. J. Anaesth.2008;101(5):610–7 .
87. Aronson JK. Nefopam . In: meyler's side effects of drugs (sixteenth edition). Oxford: Elsevier; 2016:42–3.
88. Substance Information - ECHA. 3,4,5,6-tetrahydro-5methyl-1-phenyl-1H-2,5-benzoxazocine hydrochloride.
89. Alison Ed Brayfield. Martindale: the complete drug reference. 2014:117–8.
90. J.K. Aronson. Meyler's side effects of drugs (sixteenth edition). Elsevier,2016:42-43.
91. Abou-Taleb HA, Khallaf RA, Abdel-Aleem JA. Intranasal niosomes of nefopam with improved bioavailability: preparation, optimization, and in-vivo evaluation. Drug Des Devel Ther. 2018;12:3501–16 .
92. De P, Damodharan N, Mallick S, Mukherjee B. Development and evaluation of nefopam transdermal matrix patch system in human volunteers. PDA J Pharm Sci Technol. 2009;63(6):537-546 .
93. Sukhbir S, Yashpal S, Sandeep A. Development and statistical optimization of nefopam hydrochloride loaded nanospheres for neuropathic pain using box–behnken design. Saudi Pharm J. 2016;24(5):588-99 .

94. Sukhbir Singh, Sandeep Arora, Neelam, Dharna Allawadi. Formulation, optimization and evaluation of sustained release microspheres using taguchi design. J Pharm Technol Res Manag. 2014;2(1 SE-Articles):1-12 .
95. Sharma N, Arora S, Madan J. Nefopam hydrochloride loaded microspheres for post-operative pain management: synthesis, physicochemical characterization and in-vivo evaluation. Artif Cells, Nanomedicine, Biotechnol. 2018;46(1):138-46 .
96. El-Mahdy M. Development and evaluation of nefopam hydrochloride microcapsules. Bull Pharm Sci Assiut. 2007;30(2):135-47 .
97. Uphade K. B., Patil P. B., Saudagar R. Formulation, development and in-vitro evaluation of osmotic tablet of nefopam hydrochloride . Int. J. Res. Advent Technol.2018;6(7):1672-80 .
98. The United States Pharmacopeia (USP) 41, NF36. Convention Inc. Rockville, MD. 2018.
99. S Araújo AA, Antunes Souza Araújo A, dos Santos Bezerra M, Storpirtis S, do Rosário Matos J, Bezerra MS, et al. Determination of the melting temperature, heat of fusion, and purity analysis of different samples of zidovudine (AZT) using DSC. 2010;46(1):37-43 .
100. Prichard L, Barwick V. Preparation of calibration curves a guide to best practice contact point. LGC.2003;1–27 .
101. Bhuwanesh Pratap S, Brajesh K, Kausar S. Development and characterization of a nanoemulsion gel formulation for transdermal delivery of carvedilol. J. Drug Dev. & Res. 2012;4(1):151-61 .
102. Chaudhary B, Verma S. Preparation and evaluation of novel in situ gels containing acyclovir for the treatment of oral herpes simplex virus infections. Sci World J. 2014;2014: 280928:Online .
103. Fathalla Z, Mustafa WW, Abdelkader H, Moharram H, Sabry AM, Alany RG. Hybrid thermosensitive-mucoadhesive in situ forming gels for enhanced corneal wound healing effect of L-carnosine. Drug Deliv.

2022;29(1):374-85 .

104. Begum SG, Reddy YD, Divya BS, Komali PK, Sushmitha K, Ruksar S. Pharmaceutical incompatibilites: a review. Asian J Pharm Res Dev. 2018;6(6):56–61 .
105. Nairy H, Prabhu P, Rompicherla NC, Ahmed MG, Subrahmanyam E. Formulation and evaluation of in situ gels containing clotrimazole for oral candidiasis. Indian J Pharm Sci. 2009;71:421–7 .
106. Verekar, Rucheera R. Gurav, Shailendra S. Bolmal, Udaykumar. Thermosensitive mucoadhesive in situ gel for intranasal delivery of almotriptan malate: formulation, characterization, and evaluation. Journal of Drug Delivery Science and Technology. 2020;58:101778:Online .
107. Karpagavalli L, Narayanan N, Maheswaran A, Raj A, Priya J, Kasiramar G. Formulation and evaluation of zolpidem nasal in situ gel. World J Pharm Res. 2019;6:940–51 .
108. Gonzalez-Pujana A, Rementeria A, Blanco FJ, Igartua M, Pedraz JL, Santos-Vizcaino E, et al. The role of osmolarity adjusting agents in the regulation of encapsulated cell behavior to provide a safer and more predictable delivery of therapeutics. Drug Deliv. 2017;24(1):1654–66 .
109. Dantas MGB, Reis SAGB, Damasceno CMD, Rolim LA, Rolim-Neto PJ, Carvalho FO, et al. Development and evaluation of stability of a gel formulation containing the monoterpene borneol. Sci World J. 2016;2016:7394685:Online .
110. Agrawal, Archana Maheshwari, R. K. Formulation development and evaluation of in situ nasal gel of poorly water soluble drug using mixed solvency concept. Asian Journal of Pharmaceutics. 2011;5(3):131-140.
111. Marcos L.B., Strategies to modify the drug release from pharmaceutical systems,Woodhead Publishing. 2015:63-86 .
112. Paul DR. Elaborations on the higuchi model for drug delivery. Int. J. Pharm.2011;418(1):13–7 .

113. Zhan S, Wang J, Wang W, Cui L, Zhao Q. Preparation and in vitro release kinetics of nitrendipine-loaded PLLA–PEG–PLLA microparticles by supercritical solution impregnation process. RSC Adv. 2019;9(28):16167–75 .
114. Segall A. Preformulation: the use of FTIR in compatibility studies. South Asian Academic Publications; Journal of Innovations in Applied Pharmaceutical Science 2019;4:1–6 .
115. Guerrero-Pérez MO, Patience GS. Experimental methods in chemical engineering: Fourier transform infrared spectroscopy—FTIR. Can. J. Chem. Eng.2020;98(1):25–33 .
116. Sukhbir S, Yashpal S, Sandeep A. Development and statistical optimization of nefopam hydrochloride loaded nanospheres for neuropathic pain using box–behnken design. Saudi Pharm J. 2016;24(5):588–99 .
117. Archakam SC, Chenchugari S, Sekhar C, Banoth K. Estimation of nefopam hydrochloride in bulk and parenteral dosage form by zero order and area under the curve uv spectrophotometric methods. J. Global Trends Pharm Sci. 2017;8(3):4088-95 .
118. Sharma N, Arora S, Madan J. UV-Visible spectrophotometry method validation for analysis of nefopam HCl in poly-3-hydroxybutyrate and poly-ε-caprolactone microspheres. International Journal of ChemTech Research. 2017;10(6):274-80 .
119. Soliman KA, Ullah K, Shah A, Jones DS, Singh TRR. Poloxamer-based in situ gelling thermoresponsive systems for ocular drug delivery applications. Drug Discov Today. 2019;24(8):1575–86 .
120. Jagdale S, Shewale N, Kuchekar BS. Optimization of thermoreversible in situ nasal gel of timolol maleate. Scientifica. 2016;2016:6401267:Online .
121. Alkufi HK, Kassab HJ. Formulation and evaluation of sustained release sumatriptan mucoadhesive intranasal in-situ gel. Iraqi J Pharm Sci.

2019;28(2):95–104 .

122. Stephenson FH. Solutions, mixtures, and media. in: calculations for molecular biology and biotechnology. Elsevier; 2016:15–42.
123. The United States Pharmacopeia (USP) 41, NF36. Convention Inc. Rockville, MD. 2018.
124. Adnet T, Groo AC, Picard C, Davis A, Corvaisier S, Since M, et al. Pharmacotechnical development of a nasal drug delivery composite nanosystem intended for alzheimer's disease treatment. Pharm. 2020;12(3):12030251:Online .
125. Laffleur F, Bauer B. Progress in nasal drug delivery systems. Int J Pharm. 2021;607:120994:Online .
126. Garg A, Aggarwal D, Garg S, Singla AK. Spreading of semisolid formulations: An update. Pharm. Technol. North Am.2002;26(9):84–105 .
127. Cowman MK, Schmidt TA, Raghavan P, Stecco A. Viscoelastic properties of hyaluronan in physiological conditions. F1000Research. 2015;4(622):6885.1:Online .
128. Singh RMP, Kumar A, Pathak K. Thermally triggered mucoadhesive in situ gel of loratadine: β-cyclodextrin complex for nasal delivery. AAPS PharmSciTech. 2013;14(1):412–24 .
129. Peleg M. Temperature–viscosity models reassessed. Crit Rev Food Sci Nutr. 2018;58(15):2663–72 .
130. Shau PA, Dangre P, Potnis V V. Formulation of thermosensitive in situ otic gel for topical management of otitis media. Indian J Pharm Sci. 2016;77:764–70 .
131. Kim J, Chang JY, Kim YY, Kim MJ, Kho HS. Effects of molecular weight of hyaluronic acid on its viscosity and enzymatic activities of lysozyme and peroxidase. Arch Oral Biol. 2018;89:55–64 .
132. M. PADMAA, PREETHY A., CM S., G.V. PETER. Release kinetics – concepts and applications. Int. J. Pharm. Res. Technol.2019;8(1):12-20.

133. Ricci EJ, Lunardi LO, Nanclares DMA, Marchetti JM. Sustained release of lidocaine from poloxamer 407 gels. Int J Pharm. 2005;288(2):235–44 .
134. Zhang L, Parsons DL, Navarre C, Kompella UB. Development and in-vitro evaluation of sustained release poloxamer 407 (P407) gel formulations of ceftiofur. J. Control. Release. 2002;85(1–3):73–81 .
135. Rajib, Prabina Tiwari, Deepak Srivastava, Gaurav Lever, Hindustan. Design and development of bioadhesivebuccal patches of an antidiabetic drug. WJPPS. 2018;7(8):590-605.
136. S. Manju , K. Sreenivasan. Conjugation of curcumin onto hyaluronic acid enhances its aqueous solubility and stability. Journal of Colloid and Interface Science. 2011;359(1):318-25.
137. M. Nadoura, F. Boukraa, A. Ouradia, A. Benaboura. Effects of methylcellulose on the properties and morphology of polysulfone membranes prepared by phase inversion. Materials Research. 2017;20(2):339-48.

الخلاصة

ينتمي علاج النيفوبام الى فئة الادوية غير المخدرة من مسكنات الالآم للاستخدام القصير والطويل الأمد، فئتها الكيميائية البنزوكسازوسين، ويواجه مشكلة في توافره الحيوي فيبلغ (36 %) لتكسره في الكبد. لذلك يرشح للتحضير كهلام موقعي داخل الانف لتجاوز هذه المشاكل.

تهدف هذه الدراسة الى تصييغ وتقييم هلام النيفوبام المتحسس للحرارة واللاصق بأغشية الانف المخاطية لزيادة مدة بقاء العلاج لعلاج الالآم.

تم استخدام الطريقة الباردة بإستخدام تراكيز مختلفة من البوليمر المتحسس للحرارة بولوكزامر 407 لوحده او مع البولوكزامر 188، مع البوليمرات اللاصقة بالاغشية المخاطية هيدروكسي بروبيل مثيل سليلوز، حمض الهايلورونك، كاربول 934، ومثيل سليلوز.

تم اجراء فحوصات للصيغ المصنعة وهي: حرارة ووقت تكون الهلام، مظهر الهلام، توافق المكونات بإستخدام الاشعة تحت الحمراء، الاس الهيدروجيني، ومحتوى الدواء، قوة الهلام، قابلية الانتشار، قوة التصاقه بالاغشية المخاطية، الاسمولية، اللزوجة، تحرر الدواء خارج الجسم، ثم اجريت فحوصات على الصيغ المختارة وهي محاكات تغلغل الدواء من النسيج الحيواني، توافق مكونات الصيغ بإستخدام الاشعة تحت الحمراء، ودراسة الاستقرارية للصيغ المختارة.

أظهرت النتائج ان الصيغ المرقمة (45،44،41،24،21،20،17،16،13) لديها نتائج مقبولة لفحوصات حرارة ووقت تكون الهلام، مظهر الهلام، توافق المكونات بإستخدام الاشعة تحت الحمراء، الاس الهيدروجيني، لكنها تتميز فقط بطريقة تحرر الدواء بالمقارنة مع تحرر الدواء من الصيغة المرجعية.

فقط الصيغ المرقمة (21 و45) اظهرت عدم اختلاف في تحرر الدواء عن الصيغة المرجعية.

كلتا الصيغتين اظهرت نتائج تغلغل خلال النسيج الحيواني أفضل من الصيغة المرجعية وذلك يرجع الى كون هذه الصيغ تحتوي على بوليمرات تلتصق بالاغشية المخاطية وتحسن وقت بقاء الصيغة بتماس مع النسيج الحيواني وكون هذه البوليمرات تعمل كمحسنات للتغلغل خلال النسيج.

لا يوجد اي تفاعل او عدم توافق بين النيفوبام والمواد المضافة في الصيغ كما اظهرت نتائج دراسة التوافق بإستخدام الاشعة تحت الحمراء.

يستخلص من ذلك ان بالامكان تصييغ هلام موقعي لاصق بالاغشية الانفية المخاطية ومتحسس للحرارة لعلاج النيفوبام.

جمهورية العراق
وزارة التعليم العالي و البحث العلمي
جامعة بغداد – كلية الصيدلة

صياغة وتقييم علاج النيفوبام هايدروكلورايد كهلام انفي موضعي

رسالة مقدمة الى فرع الصيدلانيات ولجنة الدراسات العليا في كلية الصيدلة|جامعة بغداد كجزء من متطلبات الحصول على درجة الماجستير في علوم الصيدلة (الصيدلانيات)

من قبل

عمار عبدالمجيد أحمد العبدلي

بكالوريوس صيدلة\جامعة الانبار (2016)

بإشراف

أ.م.د. حنان جلال كساب

1444هـ **م 2022**